Minocycline-conditioning brings surveying and reactive microglial cells to an alerted state according to their potassium channel profile

Eef Dries

promotor :
dr. Bert BRONE

co-promotor :
Prof. dr. Jean-Michel RIGO

Universiteit Maastricht

Masterproef voorgedragen tot het bekomen van de graad van
master in de biomedische wetenschappen

universiteit hasselt

Table of contents

List of abbreviations

3,4-DAP	3,4-diaminopyridine
4-AP	4-aminopyridine
aCSF	artificial cerebrospinal fluid
AD	Alzheimer's disease
ALS	Amyotrophic Lateral Sclerosis
ATP	adenosine triphosphate
CNS	central nervous system
DIC/IR	differential interference contrast/infrared
DMEM	Dulbecco's modified Eagle's medium
EAE	experimental autoimmune encephalomyelitis
E_K	equilibrium potential of potassium
E_{Ca}	equilibrium potential of calcium
FCS	fetal calf serum
g	conductance
I/V	current/voltage
I_{Ca}	calcium current
I_K	potassium current
IL	interleukin
K_{dr}	outwardly delayed rectifying potassium
K_{ir}	inwardly rectifying potassium
K_v	voltage-gated potassium
LPS	lipopolysaccharide
MAPK	mitogen-activated protein kinase
MS	multiple sclerosis
NF-KB	nuclear factor-kappaB
NO	nitric oxide
P	permeability
PS	penicillin/streptomycin
RMP	resting membrane potential
SEM	standard error of mean
SES	standard extracellular solution
SIS	standard intracellular solution
TNF-α	tumor necrosis factor α
TGF-β	transforming growth factor β
TRP	transient receptor potential
V_m	membrane potential

Acknowledgements

For 30 weeks, I have been doing my senior practical training at the department cell physiology at the biomedical research institute (BIOMED). During this period, I realized that research cannot be done alone, but is a process that needs multiple people to work together to come to the best possible result. Therefore, I want to thank the people who gave me the opportunity to do this practical training and who helped me throughout it.

In the first place I would like to thank prof. dr. Jean-Michel Rigo for giving me the opportunity to do this practical training at his department. I also want to thank him for his support and advice during all the labmeetings. Second, I would like to thank dr. Bert Brône for his daily guidance and assistance in the lab, but most of all for learning me the patch-clamp technique. Thank you for all the trust you had in me and the responsibilities you gave me in your project. I would also say some special thanks to Nina Swinnen for her advice and help with the patch-clamp, and her guidance in the animalium. Also all the other researchers of professor Rigo's department: dr. Daniel Janssen, dr. Elke Clynen, Ann Swijsen, Sheen SahebAli and Ariel Avila Macaya, thank you for all the support, the advice and the pleasant time.

Further, I also would like to say some special thanks to Katherine Nelissen en Inge Smolders who provided me the primary microglial cells for my experiments and to Silke Timmermans who helped me with the scoring of the EAE animals and the ELISA experiments. I also want to thank my second examinator, dr. Jerome Hendriks, for his advice during my internship and for critically reading my thesis. Also thanks to the other students for the mental support and the pleasant time we had during this period. At last but not least, I want to thank all my family and friends who supported me this year, but also throughout all those years.

Summary

Microglial cells, the macrophages of the central nervous system (CNS), are key players during inflammatory processes in the CNS and are characterized by the expression of several types of voltage-gated potassium (K_v) channels. Non-activated or surveying microglial cells have a linear-like current/voltage (I/V) relationship and up-regulate the inwardly rectifying potassium (K_{ir}) current, combined with a lack of an outward conductance in an early activated or alerted state. In a late activation or reactive state, microglial cells express besides their K_{ir} current, an additional strong outwardly delayed rectifying potassium (K_{dr}) current. This K_{dr} current has been reported as a physiological marker for microglial activation and is an important target to control microglial activities. In this study we investigated whether minocycline, a known microglial activation inhibitor, was able to inhibit the functional expression of this K_{dr} current. Therefore, the I/V relationships and the function of the K_v channels of primary cultured rat microglial cells were measured using the whole-cell patch-clamp technique. The I/V profiles were compared in control and lipopolysaccharide (LPS)-activated (100 ng/ml) microglial cells in absence and presence of minocycline (400 µg/ml).

Unstimulated control cells were classified into three instead of two groups: first, in contrast with the literature, occasionally cells showing a linear-like profile were observed (45%), with a small K_{ir} and a small K_{dr} current, comparable to the profile of surveying cells; second, 48% of the cells showed an increased K_{ir} current and a small K_{dr} current, comparable to the earlier described alerted cells and third, 7% of the cells showed a profile comparable to a reactive state, with a K_{ir} and a prominent K_{dr} current. Furthermore, in agreement with our hypothesis, minocycline was able to significantly decrease the K_{dr} current in LPS-activated microglial cells. However, minocycline was also able to significantly increase the K_{ir} current in control and LPS-activated cells, which has led to a **"new" I/V profile**. In addition, minocycline-conditioned control and LPS-stimulated cells also tended to be in a depolarized state, which led to a minor ATP-mediated depolarization in these cells. Since this "new" I/V profile and the depolarized resting membrane potential were comparable to that of alerted control cells, we suggested this "new" minocycline-induced phenotype to be microglial cells in an **alerted state**. Moreover, minocycline induced a I/V-profile comparable to that of IL-4-conditioned BV-2 cells and suppressed the production of pro-inflammatory cytokines (TNF-α and IL-6) in control and LPS-activated primary cultured microglial cells, indicating that the minocycline-induced phenotype was that of microglial cells in an **anti-inflammatory state**. In conclusion, these data indicated that minocycline was not able to completely inactivate microglial cells but instead brought microglial cells to an alerted state, independently of their activation history.

Samenvatting

Microglia cellen, de macrofagen van het centraal zenuwstelsel (CZS), zijn de belangrijkste elementen in neuro-inflammatoire reacties in het CZS en worden gekenmerkt door verschillende types spanningsgevoelige kalium (K_v) kanalen. Niet-geactiveerde of surveillerende microglia cellen hebben een linear-gelijkend stroom/spannings (I/V)-profiel. Deze cellen activeren een inwaartse rectificerende kalium (K_{ir}) stroom, gecombineerd met de afwezigheid van een vertraagde uitwaartse rectificerende kalium stroom (K_{dr}) in een vroeg geactiveerde of gealarmeerde toestand. In een laat geactiveerd of reactief stadium zorgen microglia cellen voor een additionele prominente K_{dr} stroom bovenop de K_{ir} stroom. Deze K_{dr} stroom is gekend als een fysiologische marker voor microglia activatie en is een belangrijk doelwit om microgliale functies te controleren. In deze studie hebben we onderzocht of minocycline, een gekende remmer van microglia activatie, in staat was om de functionele expressie van de K_{dr} stroom te onderdrukken. Om dit uit te voeren werden de I/V-profielen en de functie van de K_v-kanalen van primaire rat microglia cellen onderzocht door middel van de patch-clamp techniek in de whole-cell configuratie. Deze I/V-profielen werden vergeleken tussen controle en lipopolysaccharide (LPS)-gestimuleerde cellen (100 ng/ml) in aan- en afwezigheid van minocycline (400 µg/ml).

Niet-gestimuleerde controle cellen konden worden geklasseerd in drie groepen: (1) in tegenstelling tot de literatuur, toonde 45% van de cellen een linear-gelijkend I/V-profiel (een kleine K_{ir} en K_{dr} stroom) dat vergelijkbaar was met het profiel van surveillerende cellen; (2) 48% van de cellen toonde een stijgende K_{ir} stroom en een kleine K_{dr} stroom, dat vergelijkbaar was met het profiel van gealarmeerde cellen en (3) 7% van de cellen toonde een K_{ir} stroom en een prominent K_{dr} stroom, dat vergelijkbaar was met het profiel van reactieve cellen. Verder, in overeenstemming met de hypothese was minocycline in staat om de K_{dr} stroom significant te doen dalen in LPS-geactiveerde cellen. Maar eveneens zorgde minocycline voor een significante stijging van de K_{ir} stroom in controle en LPS-geactiveerde cellen, dat leidde tot een **“nieuw” I/V-profiel**. Verder waren de minocycline-geconditioneerde controle en LPS-geactiveerde cellen in een gedepolariseerde toestand in vergelijking met de controle cellen, wat leidde tot een kleine ATP-gemedieerde depolarisatie in deze cellen. Omdat dit nieuwe I/V-profiel en de gedepolariseerde rust membraan potentiaal vergelijkbaar waren met dat van de controle gealarmeerde cellen, suggereren wij dat dit “nieuwe” minocycline-geïnduceerde fenotype, microglia cellen in een **gealarmeerde toestand** zijn. Bovendien zorgde minocycline voor een I/V-profiel dat vergelijkbaar was met dat van IL-4 gestimuleerde BV-2 cellen en remde het de productie van pro-inflammatoire cytokines (TNF-α en IL-6). Dit toonde aan dat het minocycline-geïnduceerde fenotype dat van een microglia cel in een **anti-inflammatoire toestand** was. In conclusie geven deze resultaten aan dat minocycline niet in staat was om de microglia cellen volledig te inactiveren, maar ze naar een gealarmeerde toestand bracht, onafhankelijk van hun activatie geschiedenis.

1. Introduction

Microglial cells, the resident macrophage population of the central nervous system (CNS), are the first cells to become activated in response to pathological events, such as disease or injury in the brain [1, 2]. During this neuroinflammatory response, activated microglial cells attack the source of injury, remove damaged cells by phagocytosis and release pro-inflammatory mediators, such as tumor necrosis factor-α (TNF-α) and interleukin (IL)-6. These pro-inflammatory mediators work to perpetuate the inflammatory cycle by activating additional microglial cells, promoting their proliferation and the further release of pro-inflammatory factors [3-5]. Eventually, this reaction can result in a detrimental chronic inflammatory response, which is typical for neurodegenerative CNS disorders, such as multiple sclerosis (MS), Alzheimer's disease (AD), prion diseases, etc.. [5-7]. Nevertheless, recent evidence indicated that chronic microglial responses can also be beneficial, e.g. by the production of anti-inflammatory cytokines and trophic factors [8-10]. This functional dichotomy, either exhibiting neuroprotective or neurotoxic effects, has led to different strategies in neuroinflammatory disease therapy. The goal of these strategies can be that microglial cells that exhibit neurotoxic effects are suppressed or microglial cells that exhibit neuroprotective effects are stimulated [11]. In this study, we focused on the suppression of microglia-mediated inflammation by using minocycline, since it has been reported that minocycline was able to attenuate microglial activation and exert neuroprotective effects. However, the molecular mechanisms by which minocycline exert these inhibitory effects on microglial cells still remains unclear. Therefore, in this study we investigated whether this inactivation effect of minocycline was also represented on the functional expression of specific ion channels in microglial cells.

1.1 Microglial cells

The cellular micro-environment of the CNS comprises a network of neurons, which mediate the transmission of action potentials. Despite the essential function of neurons, 90% of the cells in the CNS are neuroglial cells. Originally, these neuroglial cells were only thought to play a passive role in the CNS, in which they acted physically to support neurons. However, now it is known that glial cells play an active role in many central homeostatic processes and also during development. In the CNS, three types of neuroglial cells are described: astrocytes, oligodendrocytes (together macroglial cells) and microglial cells (Figure 1) [1, 12].

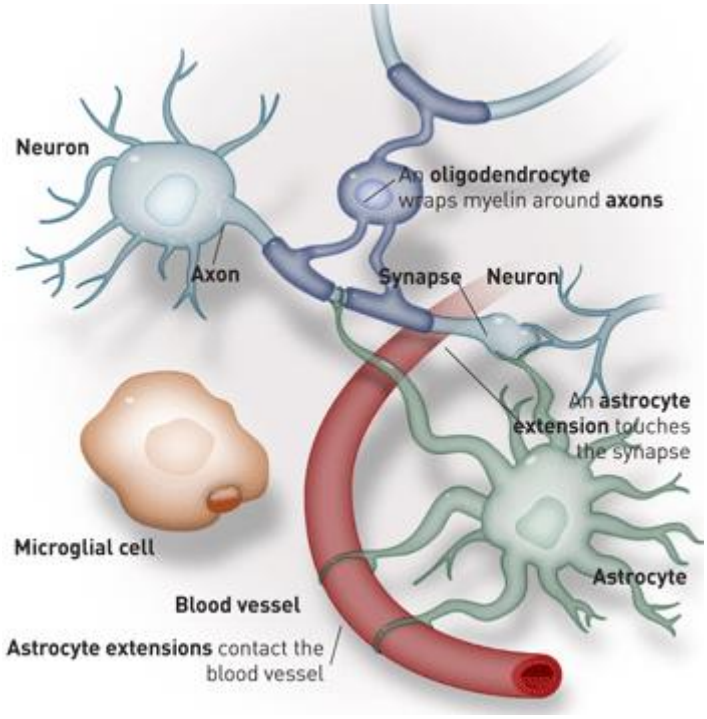

Figure 1. The different types of neuroglial cells. Neuroglial cells interact with neurons and the surrounding blood vessels. Oligodendrocytes wrap myelin around axons to speed up neuronal transmission. Astrocytes extend processes that ensheath blood vessels and synapses. Microglial cells keep the brain under surveillance for damage or infection [1].

Macroglial cells are derived from ectodermal tissue of the developing embryo, particularly the neural tube and crest, and each type has a specific function. Astrocytes play a role in the composition of the blood-brain barrier, maintenance of the extracellular ion balance and in the repair and scarring process following injuries [13, 14]. The oligodendrocytes on the other hand are responsible for the myelination of neurons in the CNS [1, 15].

Microglial cells are derived from monocytes in the blood and constitute 5-20% of the neuroglial population [16]. It was shown that the microglial precursor cells invade the CNS during development and that they are highly abundant in all regions of the CNS. However, they are less numerous in white than in gray matter [4]. The main **function** of microglial cells is to respond to pathological changes in the CNS and they are therefore called the pathological sensors of the brain [4, 17, 18]. According to their microenvironment, microglial cells are able to modify their morphology and the expression of cell surface antigens. In the normal healthy brain tissue, they are referred to as 'resting' microglial cells [4, 18]. These cells are characterized by a ramified morphology which consist of long branching processes, a small cell body and a down-regulated immunophenotype [16, 19]. However, since their processes in the resting state are constantly moving and surveying their environment, the resting microglial cells are also called 'surveying' microglial cells. During their screenings, pathological or traumatic actions can be detected and these cells rapidly transform into an activated or 'reactive'

state characterized by an amoeboid phenotype [18]. Moreover, reactive microglial cells can migrate to the site of injury, proliferate and release a variety of factors such as pro- (e.g. IL-6, IL-15, IL-8, TNF-α) and anti-inflammatory (e.g. IL-10, transforming growth factor-β (TGF-β)) cytokines and/or reactive oxygen species. In addition, reactive microglial cells become phagocytic and can present antigens [4, 18-20]. The switch from an inactivated to an activated microglia is thus accompanied by the radical alteration of microglial gene expression of structural as well as functional structures. One group of functional structures important in microglial activation is the voltage-gated potassium (K_v) channels [21, 22].

1.2 The expression of voltage-gated potassium channels in microglial cells

During microglial activation, K_v channels play an important role [21]. These channels are characterized by their selectivity for potassium (K^+) ions. Potassium will flow in or out of the cell, depending on the ion gradients and the resting membrane potential of the cell, together making up the electrochemical driving force for the ion. To understand the function of the K_v channels, the fundamental aspects of electrochemical gradients are considered first [23, 24].

1.2.1 The potassium electrochemical gradient and functional properties

The diffusion of an ion is characterized by two driving forces, the chemical and the electrical driving force. The chemical driving force is dependent on the difference in concentration of K^+ ions across the cell membrane. Because the cell has K^+ channels, K^+ can diffuse down its chemical gradient (out of the cell) since its concentration is much higher inside the cell than outside. As K^+ moves out of the cell, it leaves negatively charged proteins behind in the cell, whereas the extracellular space becomes more positively charged. This leads to a separation of charges across the cell membrane and therefore a difference in potential. This increasing potential difference (the electrical driving force) is negative inside the cell and will attract positively charged K^+ ions and as a consequence it will counteract the chemical driving force until no K^+ is flowing anymore. At this potential the two driving forces are equal to each other but opposite. This means that the K^+ currents are in equilibrium and the potential at which K^+ reaches its equilibrium is called the Nernst or equilibrium potential:

$$E_K = \frac{RT}{zF} \ln \frac{[K^+]_o}{[K^+]_i} = 2.303 \frac{RT}{F} \log 10 \frac{[K^+]_o}{[K^+]_i} \qquad (1)$$

In this equation R is the universal gas constant (8.3145 V C mol^{-1} K^{-1}), T is the absolute temperature (273.15 + T(°Celsius)), z is the charge of the ion (+1 in the case of K^+), F is faraday's constant (9.6485 x 10^4 C mol^{-1}), $[K^+]_O$ stands for the extracellular K^+ concentration (5 mM) and $[K^+]_i$ stands for the intracellular K^+ concentration (125 mM).

The Nernst equation is thus used to predict the voltage of the cell membrane if the membrane was only permeable for that specific ion. However, the cell membrane is also permeable for other ions, such as chloride (Cl^-) and sodium (Na^+). To predict the **resting membrane potential (RMP)** of the cell, the permeability (P) of the different ions has to be taken into account and therefore the Goldmann-Hodgkin-Katz equation is used (Equation 2). This indicates that the more permeable the cell membrane is for a specific ion, the closer the membrane potential the Nernst potential of that ion will reach. Most cells have a negative RMP because at rest they have far more open K^+-selective channels than Na^+ or Cl^--selective channels (Figure 2).

$$E_q = -\frac{RT}{F}\ln\left(\frac{P_{K^+}\left[K^+\right]_i + P_{Na^+}\left[Na^+\right]_i + P_{Cl^-}\left[Cl^-\right]_o}{P_{K^+}\left[K^+\right]_o + P_{Na^+}\left[Na^+\right]_o + P_{Cl^-}\left[Cl^-\right]_i}\right) \qquad (2)$$

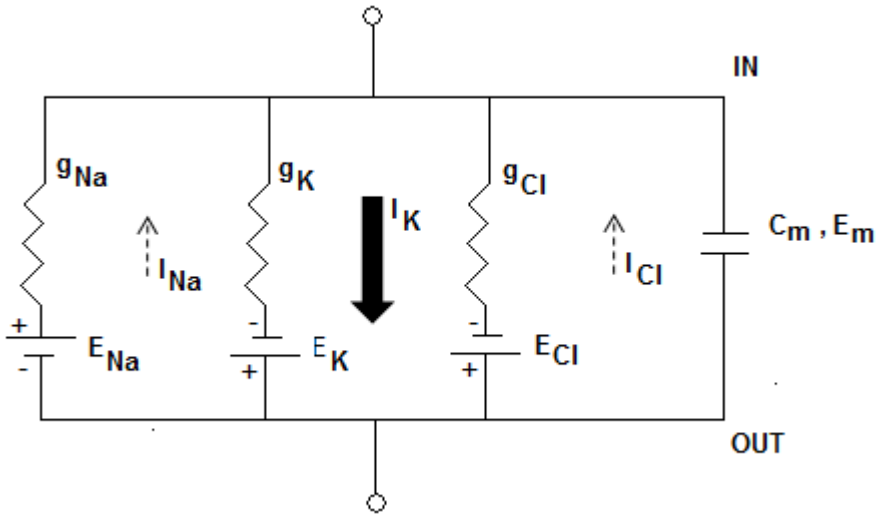

Figure 2. An equivalent electrical circuit representing the cell membrane. The driving force for each ion is represented by a battery. The potential of these batteries is the Nernst potential (E_{Na}, E_K, E_{Cl}). For each ion also the conductance is important (g_{Na}, g_K, g_{Cl}). The higher the conductance, the higher the permeability for an ion is. In rest, the conductance for K^+ is much higher than for Na^+ or Cl^-. According to Ohm's law (U = I x R), this leads to a large K^+ current and a weak Na^+ and Cl^- current. This large K^+ current eventually will charge the membrane capacity (C_m) that leads to the membrane potential (E_m). This indicates that the membrane potential, in the case of a high K^+ permeability, will reach at the Nernst potential of K^+.

According to Ohm's law (equation 3), a K^+ current (I_K) is determined by the potential difference and the conductance (g), related to the permeability.

$$I_K = g_K(V_m - E_K) \qquad (3)$$

This equation indicates that when the membrane potential (V_m) is smaller than the equilibrium potential of K^+ (E_K), I_K becomes negative, meaning that K^+ ions start flowing into the cells (Figure 3A). When the V_m is larger than the E_K, the I_K becomes more positive, indicating that the K^+ ions will start flowing out of the cell (Figure 3B). When the V_m is equal to the E_K, there is no net I_K (Figure 3C) [23].

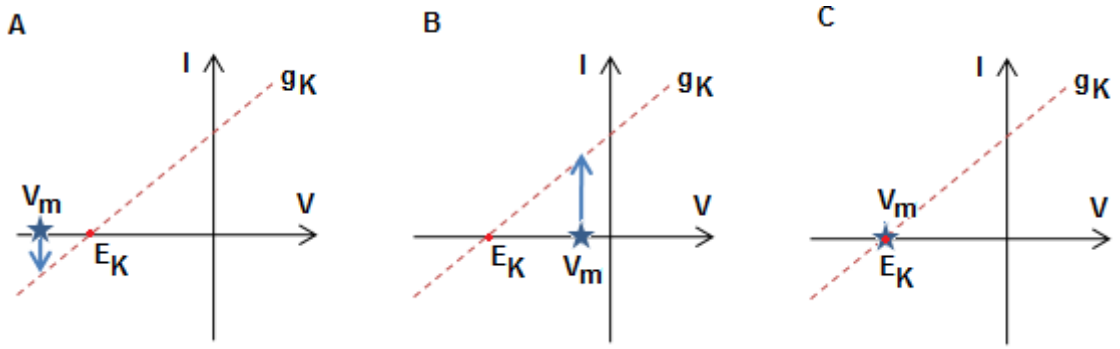

Figure 3. The I/V relationship of K^+ ions. (A) $V_m < E_K$: the K^+ current becomes negative and flows into the cell, trying to reach again the E_K. (B) $V_m > E_K$: the K^+ current becomes positive and flows out of the cell, trying to reach again the E_K. (C) $V_m = E_K$: no net K^+ is flowing. (red dot = E_K (equilibrium potential of K^+), blue star = V_m (membrane potential), dotted red line = g_K (conductance of K^+), blue arrow = I_K (K^+ current)).

In summary, since K^+ has a large membrane permeability, the membrane potential at rest in microglial cells will thus tend to the Nernst potential of K^+. This indicates that K^+ is a very important ion in the establishment of the RMP.

1.2.2 Voltage-gated potassium channels

Patch-clamp investigations have shown that K_v currents are the dominant voltage-gated ion channels in microglial cells in culture [25]. It was shown that cultured microglial cells in control conditions had a voltage-dependent inwardly rectifying K^+ conductance (K_{ir}), combined with the lack of a voltage-dependent outwardly delayed rectifying K^+ conductance (K_{dr}) (In the electrical circuit theory, the term rectification is a property describing that the membrane conductance changes in function with the voltage) [19, 26]. Moreover, when cells were stimulated with an inflammatory agent, such as lipopolysaccharide (LPS), cultured microglial cells expressed an additional K_{dr} current [19, 27, 28]. However, one of the major handicaps in studying these K_v channels in primary cultured microglial cells, is that they are always in some state of activation due to tactile stimuli and the disturbance of the normal micro-environment that occurs during cell isolation [19, 20]. Therefore, resting microglial

cells were studied in acute brain slices where they were in their natural micro-environment [19]. Within these brain slices, surveying non-activated microglial cells were characterized by little, if any, K_v channels (Figure 4A). This current pattern changes with activation of microglial cells. In an alerted state, microglial cells acquired a K_{ir} current, combined with a lack of an outward conductance (Figure 4B). In a late activation state, microglial cells expressed an additional outward K_{dr} current in isolated brain slices (Figure 4C).

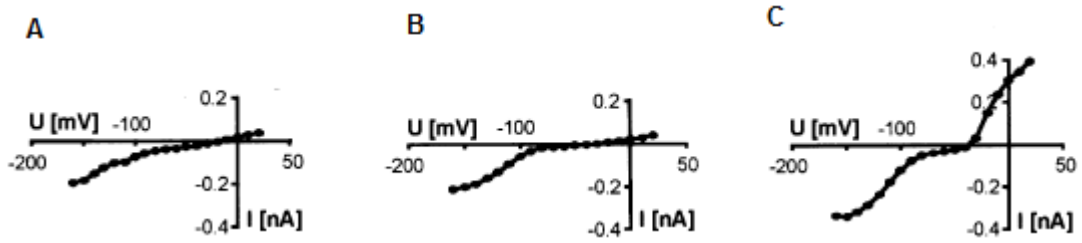

Figure 4. The I/V relationship of surveying, alerted and reactive microglial cells. (A) Surveying microglial cells showed a linear-like I/V-profile, they had a small K_{ir} and a small K_{dr} current. (B) Alerted microglial cells were characterized by the presence of a K_{ir} current and the absence of the K_{dr} current. (C) Reactive or late activated microglial cells showed a K_{ir} and prominent K_{dr} current [19].

Moreover, the appearance of K_{dr} was always associated with the induction of other activation parameters, such as inflammatory cytokines [21]. Therefore, the K_{dr} current is used as a physiological marker for microglial activation and can be a good candidate for a therapeutic target [19, 29-31]. To date, 2 broad-spectrum K^+ channel blockers, 4-aminopyridine (4-AP) and 3,4-diaminopyridine (3,4-DAP), were shown to have beneficial effects in neuroinflammatory diseases, such as in the treatment of MS [32, 33]. Although both 4-AP and 3,4-DAP produced clear neurological effects, their use has been limited due to toxic epileptogenic side effects [33-35]. These side effects raised from the indiscriminate blockade of widely distributed and varied CNS K_v channels (neurons and microglia) [33]. In that view, specific K_v blockers, either inhibiting the functionality or the gene expression, are necessary in the treatment of neuroinflammatory diseases. In this study, we investigated whether minocycline, an established inhibitor of microglial activation, was able to inhibit the functional expression of ion channels.

1.3 Minocycline

Minocycline, also known as minocycline hydrochloride, is a broad spectrum tetracycline antibiotic and is used for microbial diseases such as acne, respiratory infections and Lyme disease [36]. Aside from its antimicrobial effect, minocycline is also able to diffuse into the CNS at clinically relevant levels and exerts anti-inflammatory effects since it attenuates the inflammation associated with

microglial activation [37-41]. As reported by Henry *et al.* [42], minocycline was able to block the secretion of pro-inflammatory cytokines (IL-6 and IL-1β) of LPS-activated microglial cells. Moreover, minocycline was also able to reduce the neuroinflammatory response in several animal models of diseases with microglial involvement, such as amyotrophic lateral sclerosis (ALS) [39, 40, 43], experimental autoimmune encephalomyelitis (EAE)-induced MS [37, 38, 44] and methylphenyl-tetrahydropyridine-induced Parkinson's disease [41, 45]. However, the exact mechanism how minocycline exert its inhibitory effect on microglial cells still remains elusive.

1.4 Aim of the study

Microglial cells are the key players during an inflammatory process in the CNS. Therefore, the suppression of microglial-mediated inflammation has been considered as a major strategy in neurodegenerative disease therapy. A possible molecule for this tends to be minocycline, since it has been reported that it can inhibit microglial activation. However, the molecular mechanisms and the subsequent functional changes by which minocycline exerts its inhibitory effects on microglial cells still remains unclear. Therefore, in this study we investigated whether the inactivation effect of minocycline was also represented on the functional expression of ion channels in microglial cells. Since microglial activation has been characterized by the expression of the K_{dr} current, we hypothesized that minocycline was able to block the K_{dr} current and thus microglial activation. To investigate this, we performed voltage- and current-clamp experiments to study the I/V relationship of control and LPS-activated primary cultured microglial cells in presence and absence of minocycline. In addition, as a pilot study, the I/V relationship of microglial cells within brain slices were investigated, to evaluate the working mechanism of minocycline as a possible drug therapy. Eventually, these new insights may lead to a major contribution for the development of new drug targets for neuroinflammatory diseases such as MS.

2. Materials and methods

In this study we investigated the electrophysiological effect of minocycline on the K_v channels of microglial cells. We aimed at examining the I/V profiles and the functionality of these channels by using the patch-clamp technique. In the following sections the various procedures and patch-clamp experiments will be explained.

2.1 Microglial cell culture

BV-2 cells (a murine microglial cell line) were cultured in Dulbecco's modified Eagle's medium (DMEM; Invitrogen, Merelbeke, Belgium) with L-glutamine and a high glucose content (4500 mg/ml) (Invitrogen) without pyruvate and supplemented with 10% fetal calf serum (FCS; Invitrogen) and 100 U/ml penicillin and 100 µg/ml streptomycin (1% PS; Invitrogen). The cells were incubated in a humidified incubator at 37°C and 5% CO_2. For the experiments, BV-2 cells were seeded in Nunclon Petri dishes (35 mm, Nunc, Roskilde) at 250.000 cells/ml and incubated for 24h with 20 ng/ml IL-4. For each patch-clamp experiment, a new Petri dish with cells was taken.

Primary microglial cells were isolated from one to two day old Wistar rats (P1-P2). Rats were killed by decapitation and forebrains were isolated and mechanically dissociated. The cell homogenate was cultured for 10-12 days in poly-L-lysine-coated (5 µg/ml) cell culture flasks in DMEM with 10% FCS, 2 mM L-glutamine and 1% PS. The incubation occurred in a humidified incubator at 37°C and 5% CO_2. Microglial cells detached from the culture surface during a shake off procedure (180 rpm, 37°C, 1h) and they were subsequently collected and seeded in Nunclon Petri dishes (35 mm) at 400.000 cells/ml in DMEM with 10% FCS and 1% PS. Microglial cells were incubated in a humidified incubator at 37°C and 5% CO_2 for 1 to 3 days. For the experiments, microglial cells were incubated for 24h in different conditions: 100 ng/ml lipopolysaccharide (LPS L2143, Sigma Aldrich, Bornem, Belgium), 400 µg/ml minocycline (Sigma Aldrich), 100 ng/ml LPS and 400 µg/ml minocycline. For each patch-clamp experiment, a new Petri dish with microglial cells was taken.

2.2 Electrophysiological recordings for primary cultured and BV-2 microglial cells

The culture dish containing the microglial cells was placed on an inverted microscope and cells were continuously perfused (4-6 ml/min) at room temperature with standard extracellular solution (SES). For primary cultured microglial cells, the SES contained (in mM): 145 NaCl, 5 KCl, 1.5 $MgCl_2$, 2 $CaCl_2$, 10 HEPES, osmolarity 310 mOsm and the pH was adjusted to 7.4 with NaOH. For BV-2 microglial cells, the SES contained (in mM): 130 NaCl, 5 KCl, 2 $CaCl_2$, 1 $MgCl_2$, 10 HEPES, 10 glucose, osmolarity 305

mOsm and the pH was adjusted to 7.4 with NaOH. Micropipettes (3-4 MΩ) pulled from borosilicate capillaries (Hilgenberg, Malsfeld, Germany) were filled with standard intracellular solution (SIS). The SIS for primary cultured microglial cells contained (in mM): 125 KCl, 5 NaCl, 10 HEPES, 10 EGTA, 2 $CaCl_2$, osmolarity 290 mOsm and the pH was adjusted to 7.4 with KOH. The SIS for BV-2 microglial cells contained (in mM): 120 KCl, 1 $CaCl_2$, 2 $MgCl_2$, 10 HEPES, 11 EGTA, 10 glucose, osmolarity 290 mOsm and the pH was adjusted to 7.4 with KOH. The cells were patched in the whole-cell configuration and recordings were performed using the EPC9 HEKA amplifier (HEKA Electronik, Lambrecht, Germany). The data were recorded using PatchMaster (HEKA Electronik) and offline analysis was done with FitMaster (HEKA Electronik). In the voltage-clamp mode a gigaseal was reached, the membrane was ruptured and the membrane potential was clamped at a holding potential of -60 mV.

2.2.1 Voltage-clamp experiments

In the voltage-clamp mode, the voltage across the cell membrane was controlled and the current supplied to the circuit to hold the voltage at each level was measured. This current was equivalent to the ionic current flowing across the cell membrane in response to the voltage step. For each I/V experiment, a ramp protocol was performed whereby the voltage was gradually increased from -160 to +140 mV within 500ms. Afterwards, the voltage was again clamped at -60 mV (figure 5A). In the analysis, the current at -120 mV minus the leak current was taken as a representative value for the K_{ir} current and the K_{dr} current was represented by the current at +20 mV minus the leak current (Figure 5B). To investigate the response to adenosine-triphosphate (ATP), a second voltage-clamp protocol was used. The voltage was clamped at -60 mV and 1 mM ATP for 3s was bath-applied using the Warner SF-77B fast step superperfusion system (Warner Instruments LLC, Hamden, CT, USA) and later washed-out with SES (Figure 5C). For the analysis, the ATP-response was represented by the maximum ATP-response minus the leak current (Figure 5D).

2.2.2 Current-clamp experiments

In the current-clamp mode, the current across the cell membrane was controlled and the membrane potential was recorded. For the current-clamp experiments, the membrane current was clamped at 0 pA to measure the physiological membrane voltage in microglial cells. Next, 1 mM ATP for 3s was bath-applied using the superperfusion system and later washed-out with SES (Figure 5E). During analysis, the RMP and the maximum depolarization were determined. From this, the ATP-mediated depolarization (ΔV) was calculated by the maximum depolarization minus the RMP (Figure 5F).

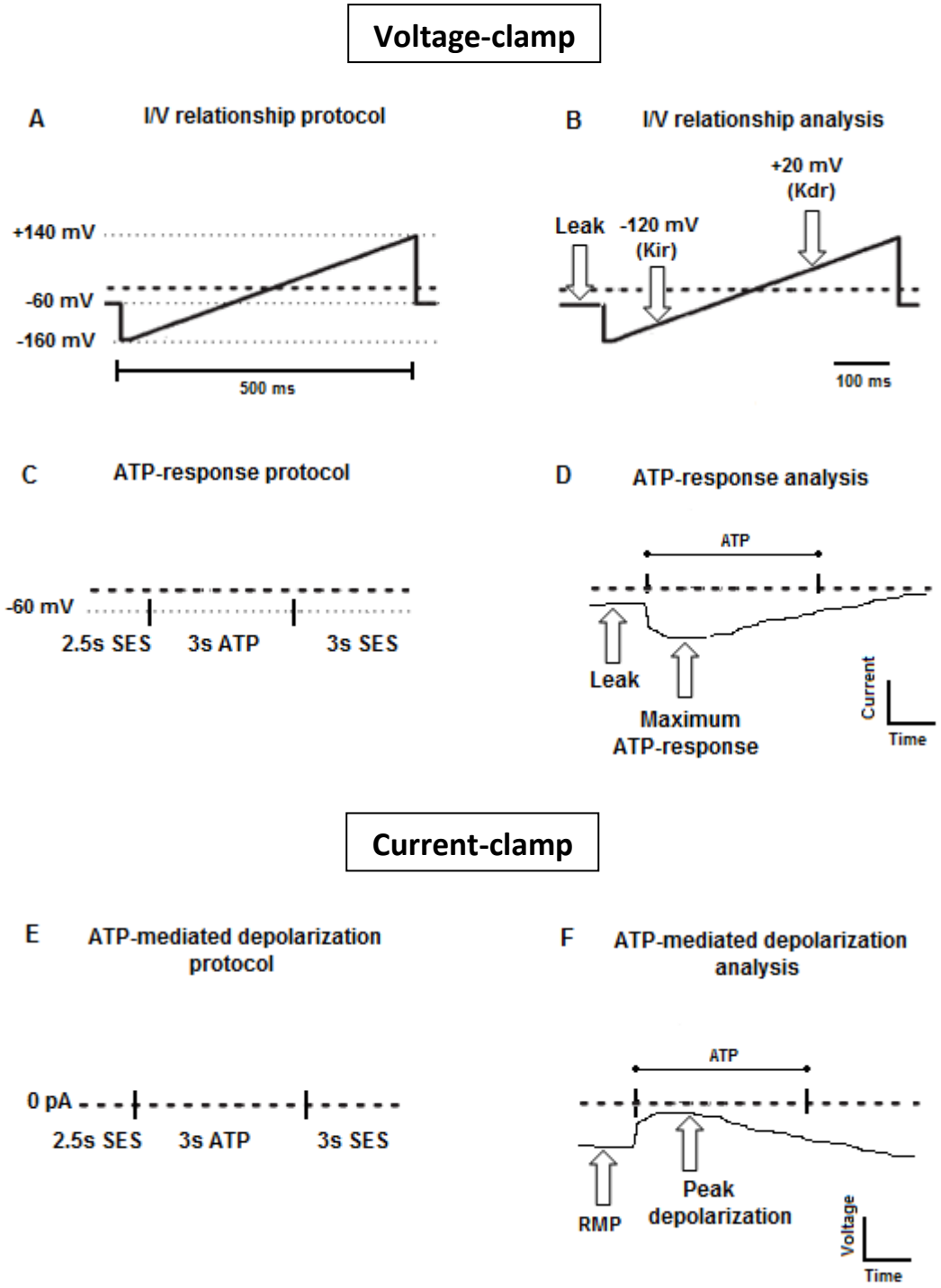

Figure 5. Patch-clamp protocols and analysis. (A) The ramp protocol as used in the whole-cell configuration voltage-clamp experiments to determine the I/V relationships. (B) The I/V relationship analysis: the arrows indicate the time points and corresponding membrane voltages at which the inwardly (K_{ir}) and outwardly delayed (K_{dr}) potassium currents and the leak currents were measured. (C) The voltage-clamp protocol used to determine the ATP-response. (D) The ATP-response analysis: the arrows indicate the leak and maximum ATP-response, and the ATP-response was calculated by the maximum ATP-response minus the leak current. (E) The ATP-mediated depolarization protocol. (F) The ATP-mediated depolarization analysis: the ATP-mediated depolarization (ΔV) was calculated by the maximum depolarization minus the RMP.

2.3 Enzyme-linked immunosorbent assay (ELISA)

After 24h of culturing the primary rat microglial cells under different control and minocycline conditions, the supernatants of the various conditions were collected and used to detect the levels of TNF-α (eBioscience kit), IL-6 and IL-10 (R&D system kit).

2.3.1 TNF-α

The ELISA plates (96 wells) were coated overnight with 100 µl/well of capture antibody in coating buffer (1/250). After washing with wash buffer (1X PBS; 0.05% tween-20), the plates were blocked with 200 µl/well 1X assay diluents and maintained on room temperature for 1h. Next, the plates were washed and 100 µl/well supernatants (1/20) was added and incubated for 2h on room temperature. After washing the plates, 100 µl/well of the detection antibody biotin-conjugate anti-rat TNF-α diluted in 1X assay diluents (1/250) was added and incubated for 1h on room temperature. Then, the plates were washed and incubated with 100 µl/well of avidine-HRP diluted in 1X assay diluents (1/250) for 30 minutes. After washing, 100 µl/well substrate solution (1X tetramethylbenzidine solution) was added and incubated for 15 min on room temperature, followed by adding 50 µl/well stop solution (2N H_2SO_4). Optical densities were measured using the Microplate Reader (Biorad Benchmark, Japan) at 450 nm and the cytokine concentrations were determined using the standard set with known concentrations of TNF-α.

2.3.2 IL-6 and IL-10

The ELISA plates (96 wells) were coated overnight with 100 µl/well of capture antibody in 1X PBS (1/180). After washing with wash buffer (1X PBS; 0.05% tween-20), the plates were blocked with 300 µl/well reagent diluent and maintained on room temperature for 1h. Next, the plates were washed and 100 µl/well supernatants was added and incubated for 2h on room temperature. After washing the plates, 100 µl/well of the detection antibody biotin-conjugate anti-rat IL-6/IL-10 diluted in reagent diluent (1/180) was added and incubated for 2h on room temperature. Then, the plates were washed and incubated with 100 µl/well of streptavidine-HRP diluted in reagent diluent (1/200) for 20 minutes. After washing, 100 µl/well substrate solution was added and incubated for 20 min on room temperature, followed by adding 50 µl/well stop solution (2N H_2SO_4). Optical densities were measured using the Microplate Reader (Biorad Benchmark, Japan) at 450 nm and the cytokine concentrations were determined using the standard set with known concentrations of IL-6/IL-10.

2.4 Animals and EAE induction

Transgenic hemizygous CX_3CR_1-/eGFP C57BL/6 mice were bred in a conventional animal facility and EAE was induced at an age of 8 weeks by subcutaneous injection of 0.1 ml MOG_{35-55} in the upper and lower back as indicated in the manual of Hooke Laboratories (Hooke Kits™ for Induction of EAE). Immediately after the subcutaneous injection, a first dose of 0.1 ml pertussis toxin was injected intraperitoneally. Within 24h, a second dose of 0.1 ml pertussis toxin was injected intraperitoneally. Mice were weighted daily and graded on scale of increasing disease severity as follows: 0 = no signs; 0.5 = partial loss of tail tone; 1 = completely limp tail; 2 = limp tail and weakness of hind legs; 2.5 = partial hind limb paralysis; 3 = complete hind limb paralysis; 4 = forelimb weakness; 5 = death. Mice were sacrificed around day 21 or the peak phase of the disease, following EAE induction and compared with age-matched hemizygous CX_3CR_1-/eGFP C57BL/6 mice.

2.5 Preparation of acute brain slices

Mice were killed by cervical dislocation, the brain was immediately removed and placed in an ice-cold sucrose cutting solution saturated with carbogene gas (5% CO_2 and 95% O_2) (in mM): 210 sucrose, 1 $CaCl_2$, 2.5 KCl, 7 $MgSO_4$, 25 glucose, 26 $NaHCO_3$, 1.25 NaH_2PO_4, pH 7.4 and osmolarity 310 mOsm. The brain was cut into 250 µm thick coronal sections with a vibratome (Microm HM 650 V, Prosan N.V., Ghent, Belgium) in ice-cold sucrose cutting solution gassed with carbogene. The brain slices were transferred to a heated (34°C) holding chamber containing an oxygenated (5% CO_2 and 95% O_2) artificial cerebrospinal fluid solution (aCSF) (in mM): 124 NaCl, 2 $CaCl_2$, 3 KCl, 10 glucose, 26 $NaHCO_3$, 1.25 NaH_2PO_4, 1 $MgCl_2$, pH 7.4 and osmolarity 310 mOsm, for 1h and then subsequently maintained on room temperature. Microglial cells in brain slices were reported to become activated within several hours [46]. To avoid the conversion from resting to activated microglia, experiments on microglial cells were performed within the first 3h after mice were killed because microglial cells tend to migrate to the cutting surface after this 3h window.

2.6 Electrophysiological recordings for microglial cells in brain slices

Individual brain slices for whole-cell patch-clamp recordings were transferred to a recording chamber mounted on a upright microscope (Nikon, JAPAN), equipped with differential interference contrast/infrared (DIC/IR) and epifluorescence optics (X-cite series 120, Exfo). Slices were continuously perfused (4-6 ml/min) at room temperature (21-24°C) with oxygenated (5% CO_2 and 95% O_2) aCSF. Micropipettes (3-4 MΩ) pulled from borosilicate capillaries (Hilgenberg) were filled with standard pipette solution containing (in mM): 120 KCl, 1 $CaCl_2$, 2 $MgCl_2$, 10 HEPES, 11 EGTA, 10

glucose, pH 7.3 and osmolarity 290 mOsm. Visually-identified eGFP-expressing microglial cells located below the slice surface were patched in whole-cell configuration and recordings were performed using the Axopatch 200B patch-clamp amplifier (Molecular Devices). The currents were collected using PClamp9 (Molecular Devices) and the offline analysis was done with PClamp10 and Graphpad Prism. To determine the I/V profile of each cell, the voltage-clamp protocol and analysis were performed, as indicated in figure 5A and B.

2.7 Statistics

Statistical analysis was done by means of one-way analysis of variance (ANOVA) with Tukey (compare all pairs of columns) or Dunnett (compare all columns versus control control) tests. Results are expressed as mean ± standard error of mean (SEM) and were considered significant when the p-value < 0.05. Statistical significance were notated by means of stars: * p-value < 0.05, ** p-value < 0.01, *** p-value < 0.001.

3. Results

Minocycline is an anti-inflammatory agent and is described to inhibit microglial activation [42]. In this study we investigated whether this inactivating effect of minocycline was also represented on the I/V profile of primary LPS-activated microglial cells. We hypothesized that minocycline was able to block the K_{dr} current of activated microglial cells. In the first part of the study the I/V relationship of control and LPS-activated primary microglial cells in presence and absence of minocycline was investigated. In the last part of this study, microglial cells within brain slices were investigated, to evaluate the working mechanism of minocycline as a possible drug therapy.

3.1 Minocycline altered the I/V relationship of primary cultured microglial cells

To study the I/V relationship of microglial cells, patch-clamp experiments in voltage- and current-clamp mode were performed with control and activated cells in presence and in absence of minocycline. To perform this, rat primary microglial cells were cultured for 24h 1) in control conditions, 2) in presence of 100 ng/ml LPS, 3) 100 ng/ml LPS and 400 µg/ml minocycline or 4) 400 µg/ml minocycline. After incubation, patch-clamp whole-cell recordings were performed with the protocols as mentioned in the materials and methods section.

3.1.1 Microglial phenotypes in the control group

Non-stimulated microglial cells can be divided into three groups, according to their I/V relationship, as studied in voltage-clamp experiments. The first group (n=13), consisted of 45% of the control cells, showed a linear-like profile between membrane potentials of -160 to +140 mV (Figure 6A & D). They showed a small K_{ir} current (-41.3 ± 8.6 pA) and a small K_{dr} current (+48.4 ± 4.9 pA) (Figure 6E). In the second group (n=14), 48% of the control cells showed a significantly increased K_{ir} current (-120.5 ± 26.9 pA, p-value < 0.05), but no change in the K_{dr} current (+65.6 ± 11.3 pA) compared to the first group of the control cells (Figure 6B, D & E). In the third group (n=2), 7% of the cells showed a K_{ir} current comparable to the second group of control cells (-188.3 ± 61.7 pA) and a significant increased K_{dr} current (+1003.7 ± 303.9 pA, p-value < 0.001), compared to the first and the second group of control cells (Figure 6C, D & E). As reported in the literature [19], microglial cells with a linear-like I/V profile (group 1) were considered to be in a surveying state. The cells expressing a K_{ir} current (group 2) were in an alerted state and the cells expressing a K_{ir} and prominent K_{dr} current (group 3) were in a reactive state. The respective names for each group were used from now on.

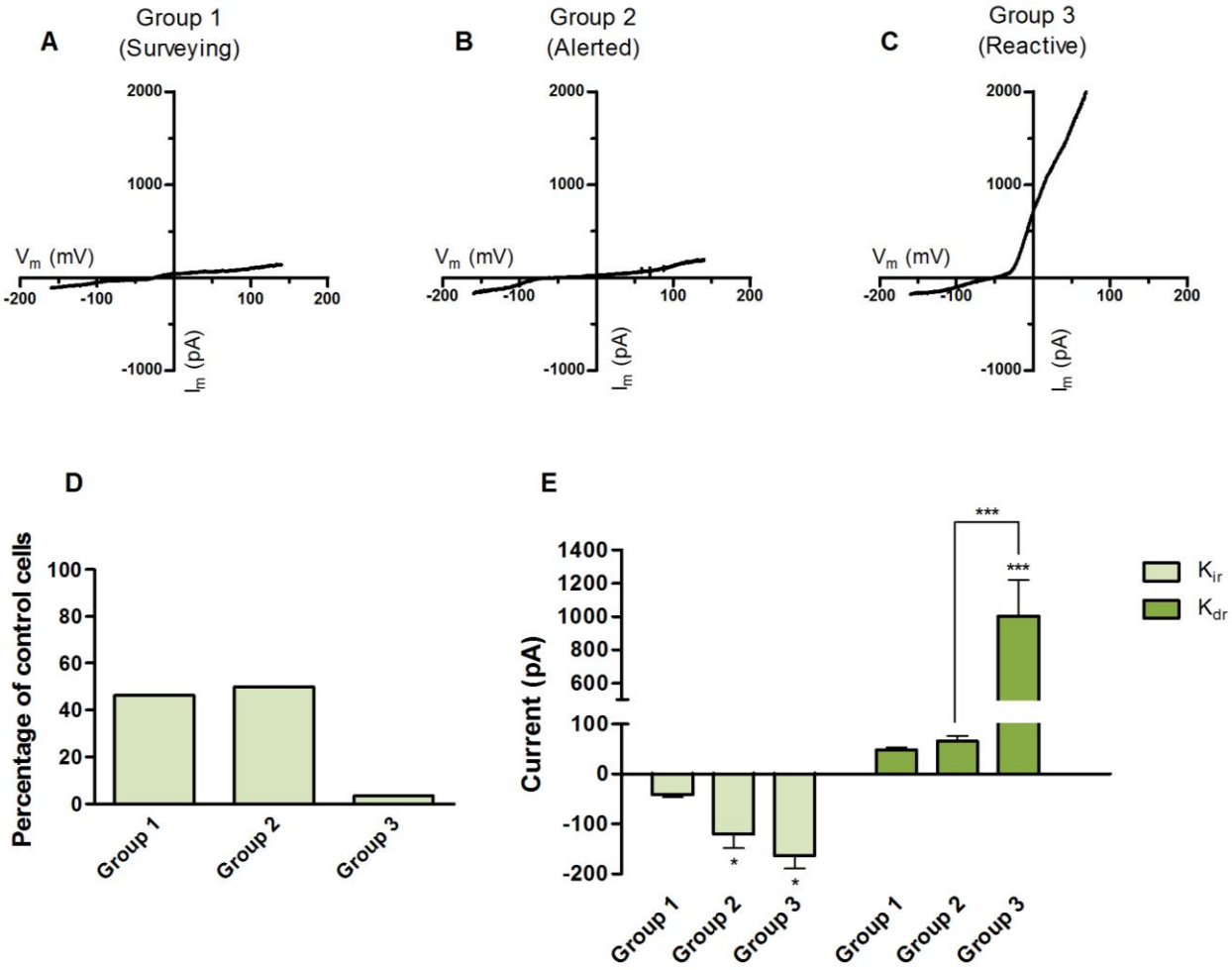

Figure 6. The I/V relationship of control primary cultured rat microglial cells. Panel A-C shows a representative current trace for each I/V profile. (D) In the control condition, an equal amount of cells were classified into group 1 and 2. Only a few cells were classified into group 3. (E) The summary of the K_{ir} and K_{dr} currents for the three control groups (Data are expressed as mean ± SEM, n = 2-14, * p-value < 0.05, *** p-value < 0.001 vs. group 1, unless indicated otherwise).

To study the function of the different K_v channels of the 3 microglial phenotypes, current-clamp experiments were performed to study the spontaneous membrane potential of microglial cells. We investigated the membrane potential (depolarization) of each group when 1 mM ATP was applied (Figure 7). These experiments confirmed the classification into three groups.

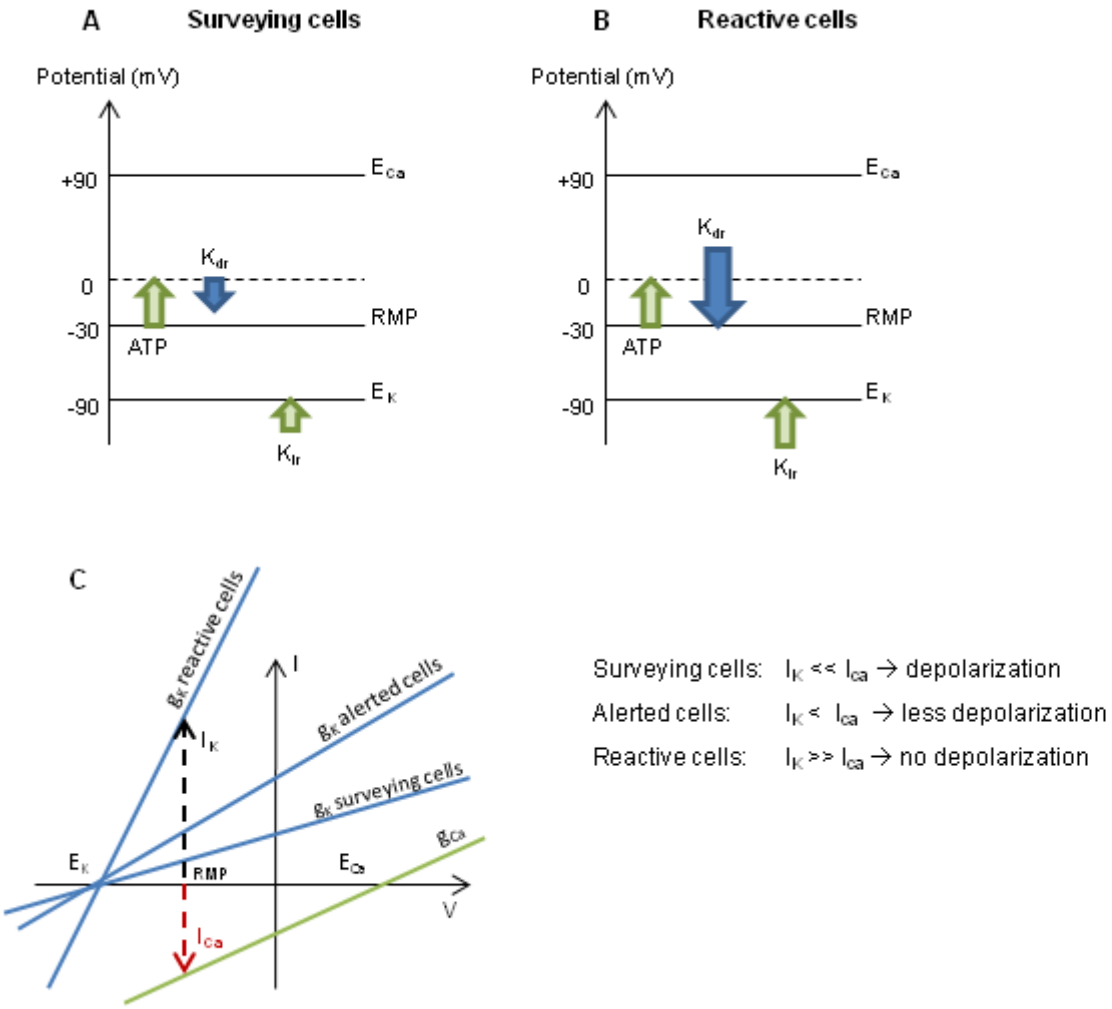

Figure 7. Theory for the ATP-mediated depolarization in microglial cells. (A) The surveying cells are characterized by a small K_{ir} and K_{dr} current that maintain the cell its negative RMP, -30 mV is taken as an example. When these cells are stimulated with 1 mM ATP, Ca^{2+} flows into the cells, shifting up the RMP towards the E_{Ca}, leading to a depolarization of the cell membrane. This membrane depolarization can be detected during the current-clamp when 1 mM ATP is applied (B) The reactive cells are characterized by a small K_{ir} and a very prominent K_{dr} current to keep the cell at its RMP. When cells are stimulated with 1 mM ATP, a positive current flows into the cell, trying to depolarize the cell. However, this depolarization is attenuated since the K_{dr} current is so large that it immediately counteracts the ATP-mediated depolarization of the cell. (C) In summary, when ATP binds to its purinergic receptor, the receptor becomes activated and Ca^{2+} ions will flow into the cell. However, dependent on the conductance of K^+ (g_K), the K_{dr} current will be larger or smaller and allow a membrane depolarization or not when ATP is applied. When cells have a small g_K, and thus a small K_{dr} current, the ATP-mediated Ca^{2+} current (I_{Ca}) will be larger than the K^+ current (I_K) and leads to a depolarization. In the cells that have a large g_K, and thus a large K_{dr} current, the I_K will be much larger than the I_{Ca}, which leads to no depolarization. (green line = conductance of Ca^{2+}; blue line = conductance of K^+; red striped line = Ca^{2+} current; black striped current = K^+ current).

Dependent on their I/V profiles, the control surveying microglial cells (n=2) showed a RMP of -65.1 ± 2.1 mV and depolarized to -34.7 ± 3.3 mV when 1 mM ATP was applied (Figure 8A & D). In the control alerted microglial cells (n=10), the RMP was -22.9 ± 5.4 mV and depolarized to -13.2 ± 4.7 mV when 1 mM ATP was applied (Figure 8B & D). In the reactive microglial cells (n=2), the RMP was -73.3 ± 12.3

mV and in the presence of 1 mM ATP they depolarized to -72.7 ± 12.4 mV (Figure 8C & D). These results showed that the RMP of the control alerted microglial cells was significant lower than the control surveying or the control reactive cells (p-value < 0.05) (Figure 8D). Moreover, the ΔV was significant lower in the control alerted compared to control surveying cells (p-value < 0.001) and in the control reactive compared to control alerted cells (p-value < 0.01) (Figure 8E), which indicated that the proposed working mechanism as explained in figure 7 was true. From now on, control cells were considered to have a linear-like profile as in the control surveying cells when compared to other conditions.

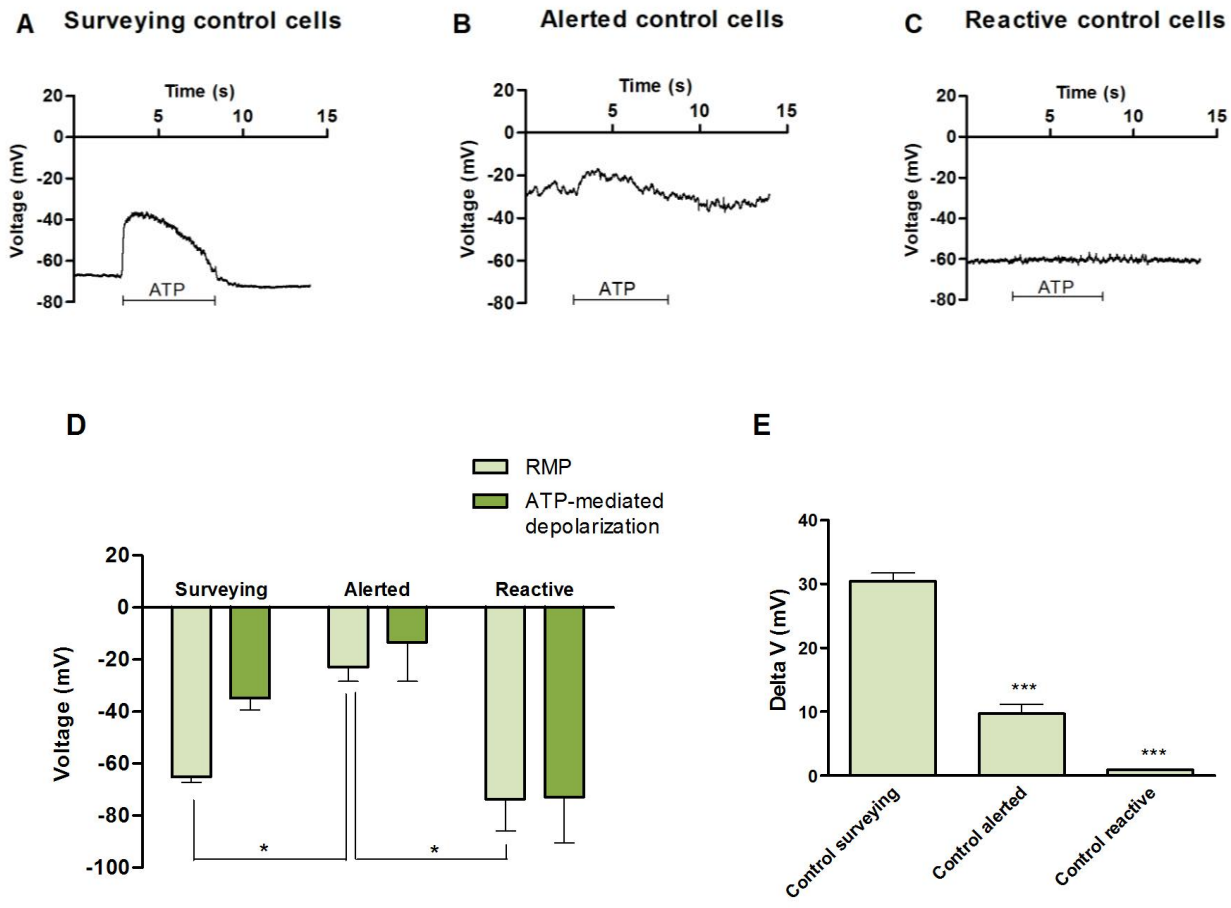

Figure 8. The ATP-mediated membrane depolarization of control primary cultured rat microglial cells. Panel A-C shows a representative current-clamp trace based on their I/V profile. (D) The RMP of the control alerted microglial cells was significant lower than the control surveying or the control reactive cells (For all the groups the RMP and the ATP-mediated depolarization is given). (E) The delta V was significant lower in the control alerted and control reactive cells compared to the control surveying cells. (Data are expressed as mean ± SEM, n = 2-10, * p-value < 0.05, *** p-value < 0.001 vs. control surveying cells, unless indicated otherwise).

3.1.2 Pro- and anti-inflammatory stimuli change the I/V profile of primary cultured microglial cells

When the cells were stimulated for 24h with LPS (n=16), microglial cells showed an increase in the K_{ir} current (-119.1 ± 42.7 pA) and a very prominent K_{dr} current (+611.3 ± 109.5 pA) compared to the control cells (Figure 9B). In agreement with our hypothesis, cells stimulated with 24h of LPS and minocycline (n=21) showed a suppressed K_{dr} current (+119.1 ± 20.6 pA) compared to the cells stimulated 24h with LPS. However, these cells also had a prominent increase in the K_{ir} current (-334.3 ± 38.3 pA) compared to LPS-stimulated cells (Figure 9C). Stimulation with 24h of minocycline (n=13) alone, also had an effect on the electrophysiological profile: it increased the K_{ir} current (-217.3 ± 31.7 pA), but did not have an effect on the K_{dr} current (+67.6 ± 10.7 pA), compared to the control cells (Figure 9D).

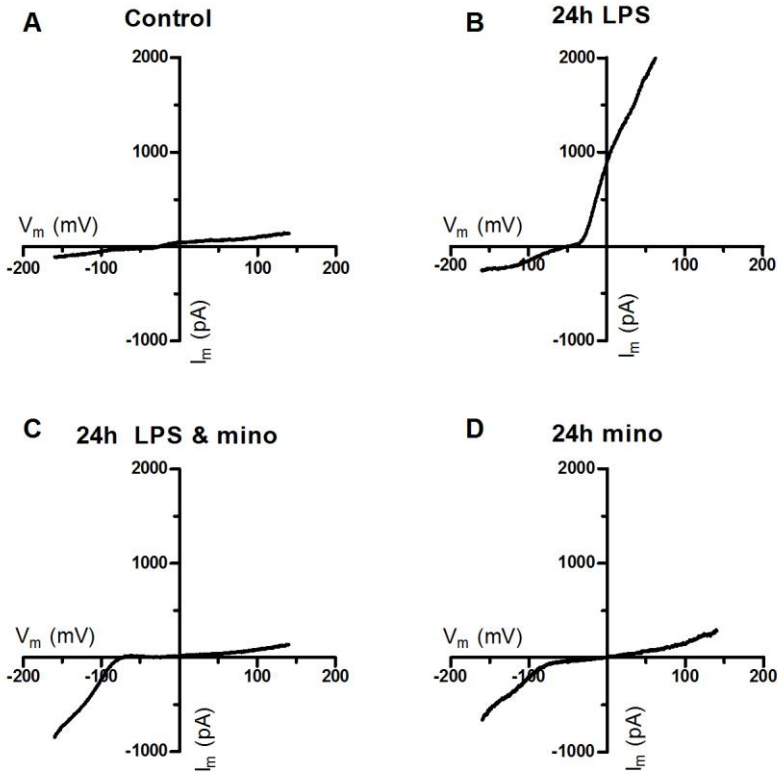

Figure 9. The I/V relationship of control and LPS-activated primary cultured rat microglial cells in presence and absence of minocycline. Panel A-D shows a representative current trace for each I/V profile.

These results indicated that minocycline significantly decreased the K_{dr} current in LPS-activated microglial cells (p-value < 0.001) and significantly increased the K_{ir} current in control (p-value < 0.05) and LPS-activated cells (p-value < 0.05) (Figure 10).

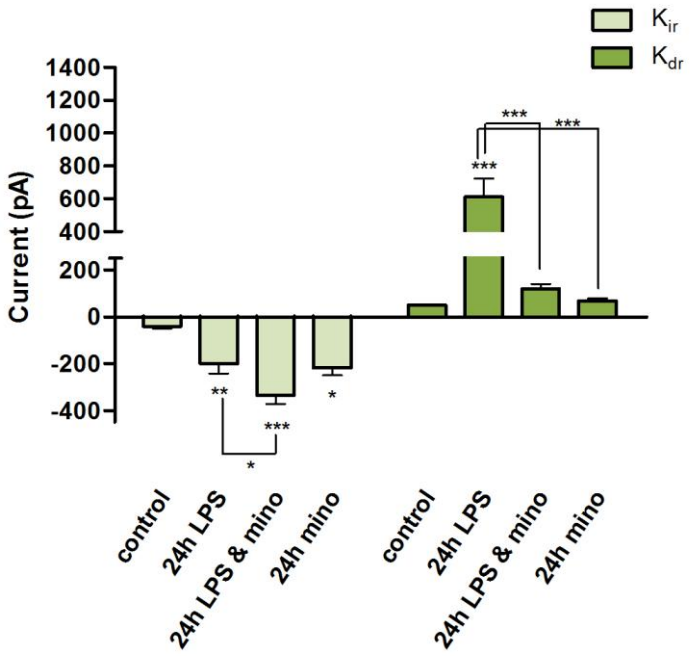

Figure 10. The summary of the I/V relationship of control and LPS-activated primary cultured rat microglial cells in presence and absence of minocycline. Minocycline-conditioning suppressed the K_{dr} current in LPS-activated microglial cells and increased the K_{ir} current in LPS-activated and control microglial cells (Data are expressed as mean ± SEM, n = 13-21, * p-value < 0.05, ** p-value < 0.01, *** p-value < 0.001 vs. control, unless indicated otherwise).

Current-clamp experiments were performed to study the function of the K^+ channels on these minocycline-conditioned microglial cells as indicated in figure 7. Microglial cells stimulated 24h with LPS (n=13) showed a RMP of -56.9 ± 6.1 mV and depolarized to -53.7 ± 6.5 mV in presence of 1 mM ATP (Figure 11B & E). After 24h stimulation with LPS and minocycline, microglial cells (n=8) showed a RMP of -5.2 ± 4.2 mV and in presence of 1 mM ATP they depolarized to -2.5 ± 4.1 mV (Figure 11C & E). The microglial cells stimulated 24h with minocycline (n=9) showed a RMP of -9.9 ± 8.2 mV and depolarized to -9.1 ± 8.2 mV in presence of 1 mM ATP (Figure 11D & E). These results indicated that the RMP of the cells stimulated 24h with LPS and minocycline and the cells stimulated 24h with minocycline alone, was significantly lower than the control cells (p-value < 0.01 vs. LPS & mino; p-value < 0.05 vs. mino) and the cells stimulated for 24h with LPS (p-value < 0.001 vs. LPS & mino and mino) (Figure 11E). This indicated that the cells stimulated with minocycline remained in a more depolarized state compared to the control or LPS-stimulated cells. Moreover, in contrast with our theory in figure 7, the ΔV was significant lower in the cells stimulated 24h with LPS and minocycline and minocycline alone, compared to the control cells (p-value < 0.001) (Figure 11F).

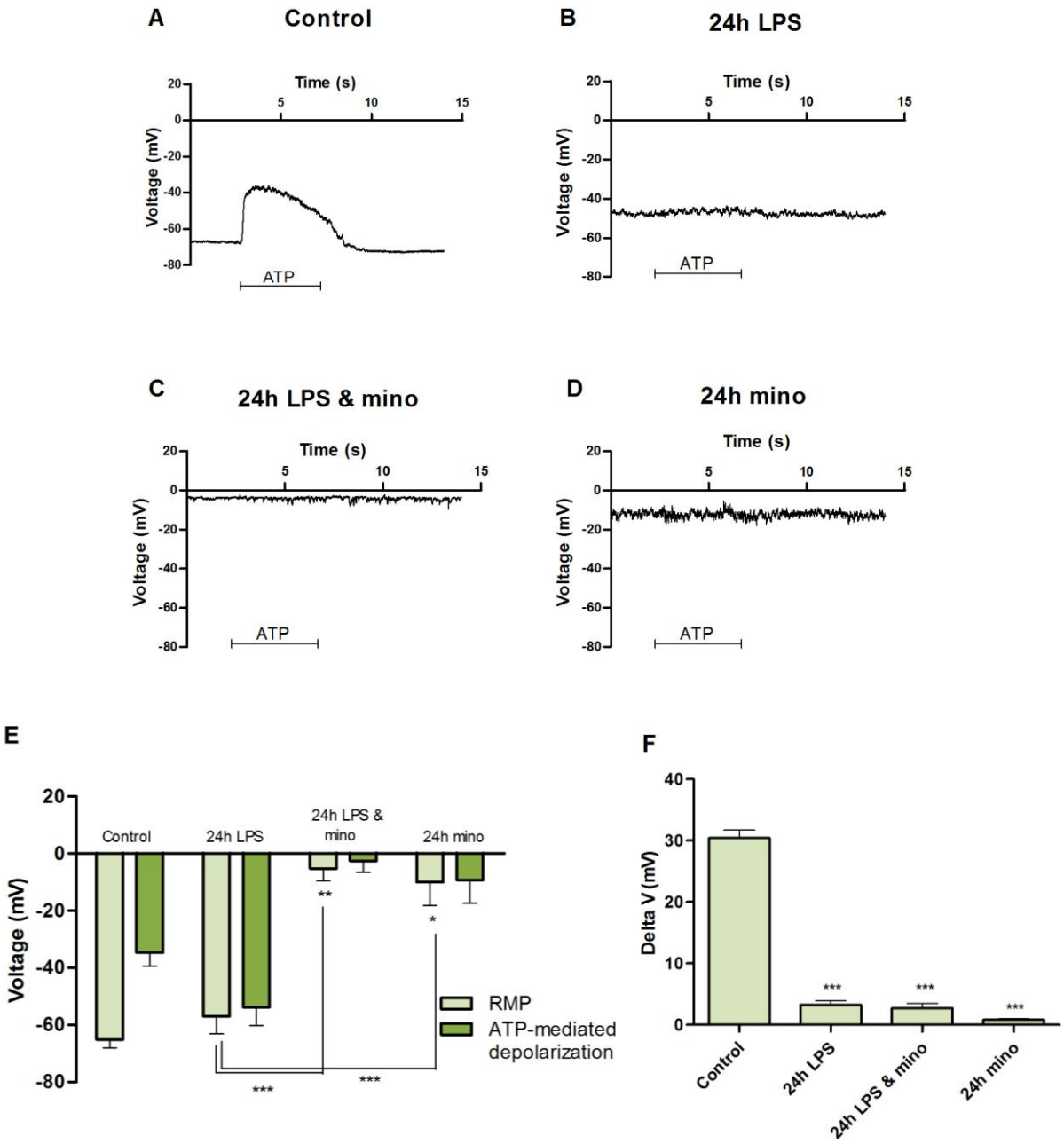

Figure 11. The summary of the ATP-mediated membrane depolarization of control and LPS-activated primary cultured rat microglial cells in presence and absence of minocycline. Panel A-D shows a representative current-clamp trace for each condition. (D) Minocycline-conditioned control and LPS-activated cells showed a higher RMP compared to the control and LPS-activated cells (For each group the RMP and the ATP-mediated depolarization is given). (E) Minocycline-conditioned cells had a significant lower delta V compared to the control cells (For each group the delta V is given) (Data are expressed as mean ± SEM, n = 2-13, * p-value < 0.05, *** p-value < 0.001 vs. control, unless indicated otherwise).

To understand the absence of an ATP-induced depolarization in minocycline-conditioned cells, we investigated their response to ATP. In the control condition, microglial cells (n=9) showed an ATP-response of -17.3 ± 3.1 pA. The cells stimulated 24h with LPS (n=6) showed a response comparable to

the control cells. They had an ATP-response of -11.1 ± 3.7 pA. The cells stimulated 24h with LPS and minocycline (n=9) showed an ATP-response of -4.7 ± 1.7 pA, which was significantly lower compared to the control cells (p-value < 0.01) and LPS-stimulated cells (p-value < 0.05). Stimulation 24h with minocycline alone (n=9), resulted in an ATP-response of -8.8 ± 1.6 pA, which was significantly lower compared to the control cells (p-value < 0.05) (Figure 12).

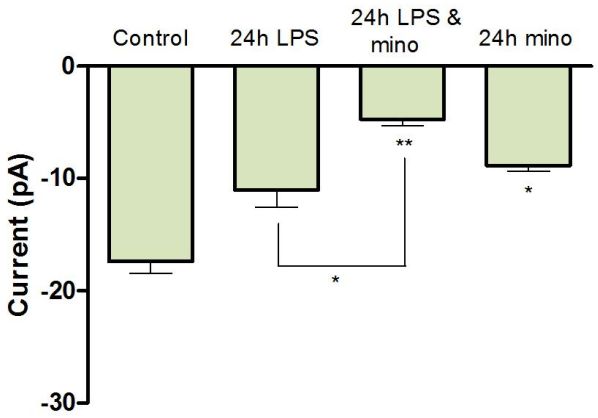

Figure 12. The ATP-response in control and LPS-activated primary cultured rat microglial cells in presence and absence of minocycline. Minocycline-conditioned control and LPS-activated cells had a significant reduction of the ATP-response when compared to the control and LPS-activated microglial cells (Data are expressed as mean ± SEM, n = 6-9, * p-value < 0.05, ** p-value < 0.01 vs. control, unless indicated otherwise).

3.1.3 Minocycline induced a phenotype comparable to that of the control alerted cells

The previous data indicated that the cells stimulated 24h with LPS and minocycline and with minocycline alone showed I/V profiles comparable to that of the control alerted cells. The cells stimulated 24h with minocycline alone neither showed significant differences in the K_{ir} current nor in the K_{dr} current compared to the control alerted cells (Figure 13A). However, the K_{ir} current in cells stimulated 24h with LPS and minocycline was significant higher compared to the control alerted cells (p-value < 0.001) (Figure 13A). In addition, the cells stimulated 24h with LPS and minocycline and minocycline alone showed comparable RMPs (Figure 13B), but had a significant lower ΔV compared to the control alerted cells (p-value < 0.001) (Figure 13C). Moreover, minocycline-conditioned cells also showed a significant lower ATP-response compared to the control alerted cells (Figure 13D).

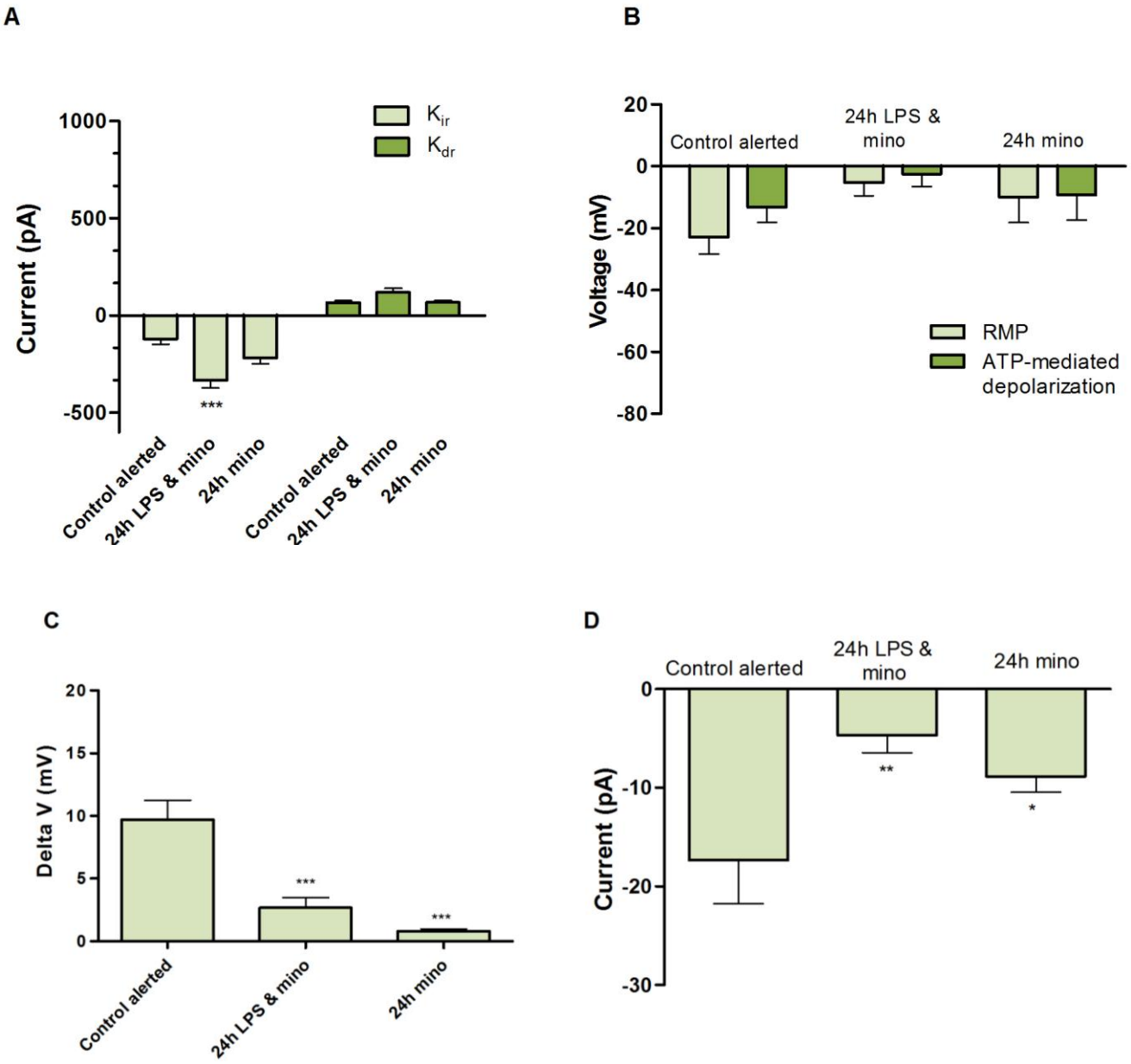

Figure 13. The summary of the comparison of control alerted and minocycline-conditioned primary cultured rat microglial cells. Minocycline-conditioned cells showed a I/V profile (A) and a RMP (B) comparable to that of the alerted control cells. The delta V (C) and the ATP-response (D) were significant lower in the minocycline-conditioned cells compared to the control alerted cells (Data are expressed as mean ± SEM, n = 8-21, * p-value < 0.05, ** p-value < 0.01, *** p-value < 0.001 vs. control alerted cells).

In summary, these data indicated that minocycline suppressed the K_{dr} current in LPS-activated microglial cells and increased the K_{ir} current in LPS-activated and control microglial cells. In addition, in this minocycline-induced phenotype, the control and LPS-activated cells tended to be in a depolarized state and showed a lower ATP-response compared to the control surveying cells. Moreover, minocycline-conditioning induced a microglial phenotype comparable with the control alerted cells, since they showed comparable I/V profiles and RMP. This indicated that minocycline was not able to fully inactivate microglial cells, but instead brought them to an alerted state.

3.2 Minocycline induced a I/V prolife comparable to that of IL-4-conditioned BV-2 cells

To investigate whether this minocycline-induced alerted state an anti-inflammatory phenotype is, we compared the I/V profiles of minocycline-conditioned cells with BV-2 cells stimulated with IL-4, an anti-inflammatory cytokine that is able to induce an anti-inflammatory phenotype in microglial cells [47]. For this experiment, BV-2 microglial cells were 24h incubated with IL-4 (20 ng/ml) and patch-clamp experiments in the voltage-clamp mode were performed. The I/V-profiles of minocycline-conditioned primary LPS-activated (n=21, Figure 14A) and control (n=13, Figure 14B) microglial cells were comparable to the I/V profile of the BV-2 cells stimulated 24h with IL-4 (n=6, Figure 14C). Moreover, no significant differences were observed in the K_{ir} and K_{dr} currents between the different conditions (Figure 14D).

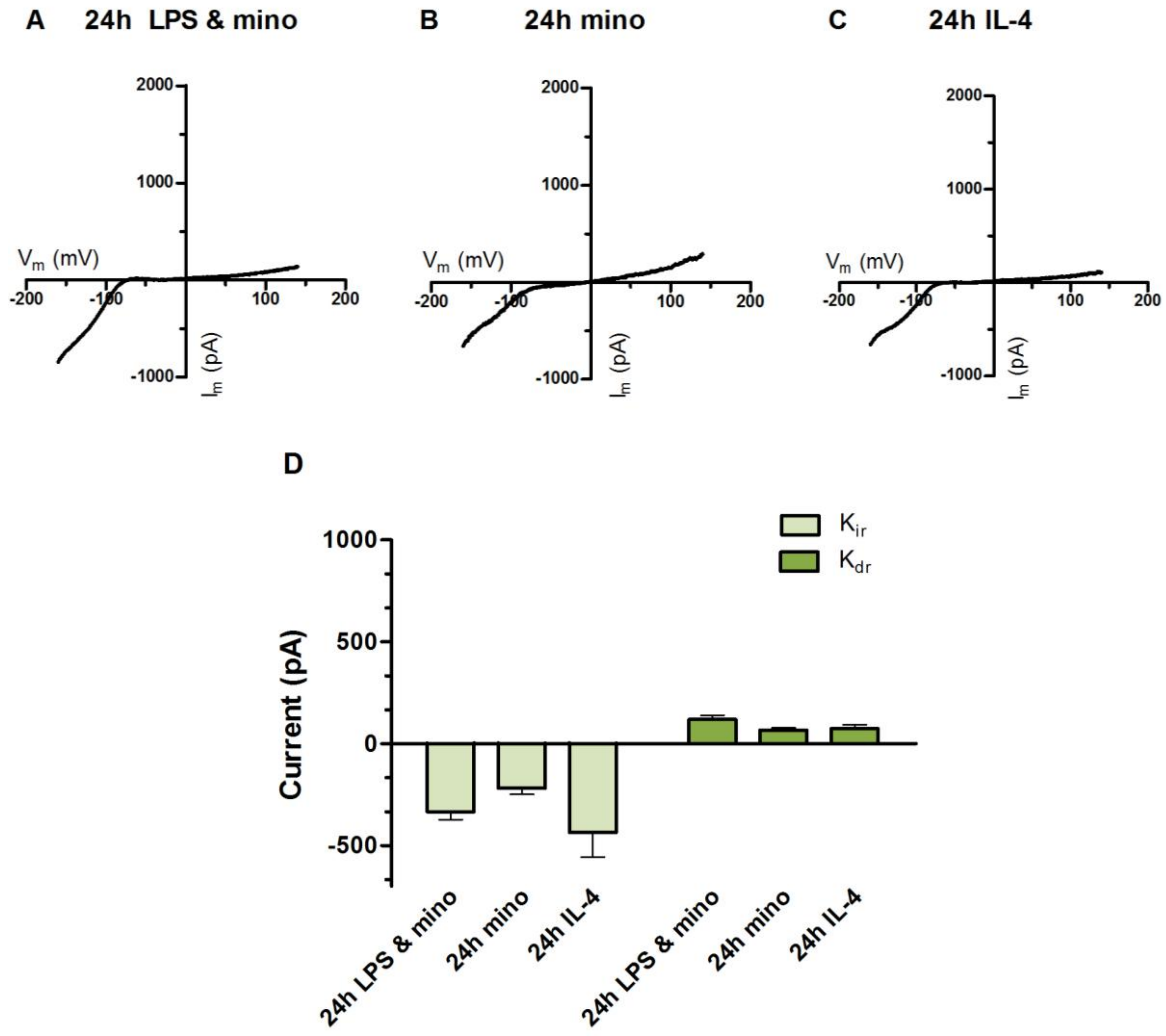

Figure 14. The comparison of the I/V-profiles of minocycline-conditioned primary cultured rat microglial cells and IL-4-conditioned BV-2 cells. Panel A-C shows a representative current trace for each I/V profile. (D) The I/V profiles of the minocycline-conditioned primary rat microglial cells were comparable to that of the IL-4-conditioned BV-2 cells, since no significant differences were observed between the K_{ir} and K_{dr} currents (Data are expressed as mean ± SEM, n = 6-21).

3.3 Minocycline suppressed the secretion of pro- and anti-inflammatory cytokines

To confirm that the minocycline-induced phenotype was of an anti-inflammatory type, we investigated the cytokine-production of primary cultured microglial cells in presence and absence of minocycline by means of an ELISA assay. In this experiment (n=1), we investigated the cytokine-production of both pro- (TNF-α and IL-6) and anti- (IL-10) inflammatory cytokines. Stimulation with 24h of LPS significantly increased the production of TNF-α (p-value < 0.05) and IL-6 (p-value < 0.01) compared to the control cells (Figure 15A & B). In contrast, stimulation with minocycline significantly reduced the production of TNF-α in the cells stimulated 24h with LPS and minocycline compared to the cells stimulated with LPS alone (p-value < 0.05) (Figure 15A). Also, the production of IL-6 was significant lower in the cells stimulated 24h with LPS and minocycline (p-value < 0.001) and minocycline alone (p-value < 0.05) (Figure 15B). Moreover, IL-10 could not be detected in the minocycline-conditioned cells, indicating that minocycline probably reduced the production of IL-10 significantly (Figure 15C).

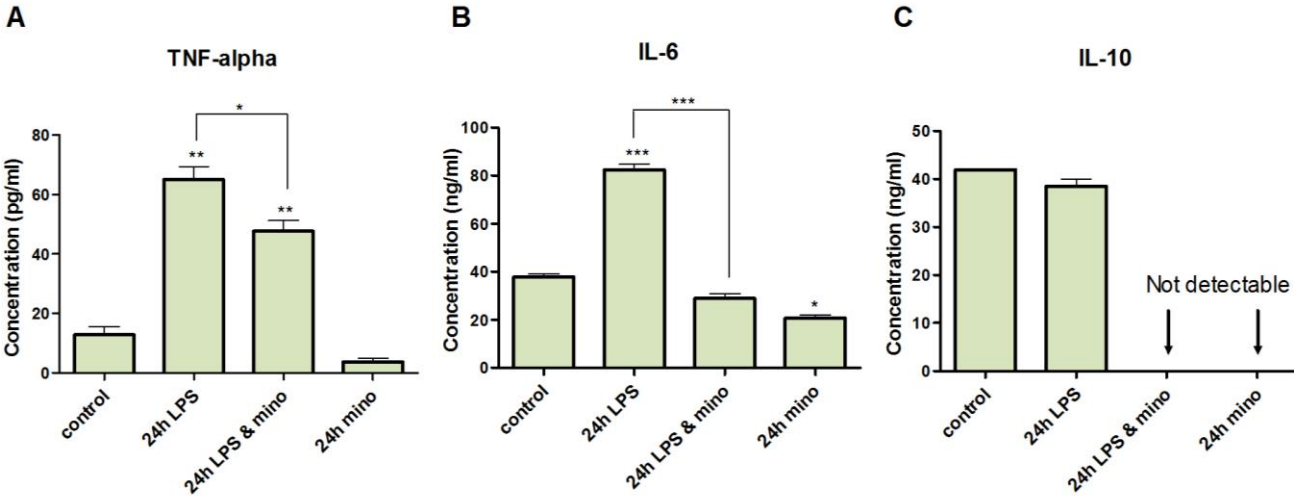

Figure 15. The cytokine-production of primary cultured rat microglial cells in presence and absence of minocycline. The production of TNF-α (pg/ml), IL-6 (ng/ml) and IL-10 (ng/ml) were significant decreased in the minocycline-conditioned control and LPS-activated cells (Experiments were performed in duplo and data are expressed as mean ± SEM, n = 2, * p-value < 0.05, ** p-value < 0.01, *** p-value < 0.001 vs. control, unless indicated otherwise).

3.4 Pilot study: the electrophysiological profiling of microglial cells in situ

As a pilot study, we also investigated the I/V profiles of microglial cells within brain slices, which enabled us to study the microglial cells in their natural micro-environment. For this experiment we used control and EAE-induced hemizygous CX_3CR_1-/eGFP C57BL/6 mice, from which we made brain slices and performed patch-clamp experiments on the eGFP-expressing microglial cells. In the control animals, the microglial cells showed a linear-like profile (n=4). They showed a small K_{ir} current (-41.1

± 6.7 pA) and a small K_{dr} current (+28.9 ± 19.1 pA) (Figure 16A). In a brain lesion of an EAE-induced mice, we found a microglial cell (n=1) with a K_{ir} current (-111.5 pA) and a small K_{dr} current (+47.1 pA) (Figure 16B) and a microglial cell (n=1) with a K_{ir} (-165.1 pA) current and a prominent K_{dr} current (+131.1 pA) (Figure 16C).

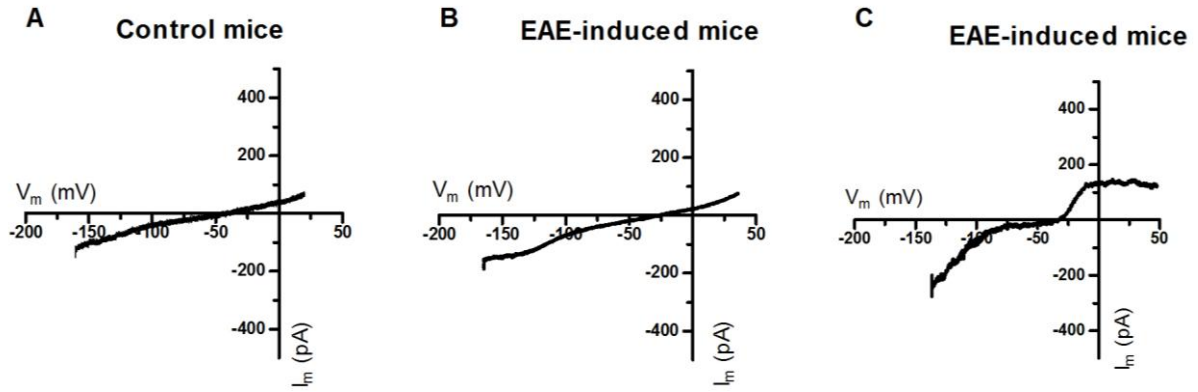

Figure 16. The I/V profiles of microglial cells within brain slices of a control and EAE-induced transgenic mice. Panel A-C shows a representative current trace for microglial cells in a control animal (A) and in an EAE-induced animal (B-C).

4. Discussion

Microglial activation is one of the hallmarks in neuroinflammation and has been observed in several neurodegenerative diseases such as for example MS and AD. In this activation process, K_v channels play a pivotal role [35]. As shown by Kettenmann *et al.* [26], primary cultured and in situ activated microglial cells showed a K_{ir} current, combined with a prominent K_{dr} current. Moreover, the appearance of the K_{dr} current was always associated with the induction of other activation parameters, like the secretion of pro-inflammatory cytokines, and has therefore been reported as a physiological marker for microglial activation [19]. As a result, targeting this K_{dr} current could lead to the inactivation of microglial cells and beneficial effects in neuroinflammatory diseases as is shown by the beneficial effect of 4-AP. Yet, 4-AP showed adverse effects due to its aspecific effect on many K_v-subtypes [23, 34]. In this study, we investigated whether the inactivating effect of minocycline was reflected in the functional expression of K_v channels. We investigated the I/V relationship in control and LPS-activated primary cultured rat microglial cells, in presence and in absence of minocycline.

4.1 Microglial phenotypes in the control group

At first we found, in contrast to the literature, that control primary cultured rat microglial cells could be divided into three instead of two categories, based on their I/V relationship: cells showing a linear-like I/V profile, cells expressing a K_{ir} current and cells showing a K_{ir} together with a prominent K_{dr} current. To confirm the presence of this K_{ir} current in the last two groups, preliminary results indicated that this inward current could be blocked with 100 µM Ba^{2+}, an extracellular inhibitor of the K_{ir} channels (data not shown). Moreover, this I/V-based classification corresponded to the three microglial types found during a facial nerve section in situ, as reported by Boucsein *et al.* [19]. Therefore, these results suggested that control cells that showed a linear-like profile were surveying microglial cells, cells that expressed a K_{ir} current were in an alerted state and the additional expression of a prominent K_{dr} current was indicative for reactive microglial cells [18, 19]. This I/V-based classification was also found with current-clamp experiments in which we measured the membrane depolarization upon ATP-stimulation. In agreement with our theory in figure 7, the cells with a linear-like I/V profile (surveying cells) tended to depolarize more upon ATP stimulation than the alerted cells with a K_{ir} current, since the driving force of Ca^{2+} was higher than that of K^+. In the alerted cells, the driving force of Ca^{2+} was a little higher than that of K^+, which led to a minor depolarization and in the reactive cells, the driving force of K^+ was much higher than that of Ca^{2+}. This resulted in no ATP-mediated depolarization, since the K^+ ions were able to counteract the positive charges of Ca^{2+} that tried to depolarize the cell membrane.

In addition, as reviewed by Judge *et al.* [35], microglial cells expressed between their unstimulated and reactive states, the outwardly delayed rectifying potassium Kv1.5 current. Therefore, the small voltage-dependent K_{dr} current in surveying and alerted microglial cells might be a Kv1.5-like current. Moreover, as reported by Menteyne *et al.* [29], the prominent K_{dr} current in reactive cells might be a Kv1.3-like current since Kv1.3 channels predominantly determine the K_{dr} current in reactive microglial cells. As suggested by Judge *et al.* [34], the K_{ir} current, both in early and fully activated microglial cells, tended to be mediated by the Kir2.1 channel [35]. This suggests that the K_{ir} in the alerted and reactive state tends to be a Kir2.1-like current. However, more pharmological tests, polymerase chain reactions (PCR) or immunohistochemical assays need to be performed to indicate the presence of these specific K_v channels in these different types of control microglial cells.

In summary, we classified primary cultured rat microglial cells in control conditions into three categories, in which we detected an equal amount of cells that were in a surveying or an alerted state and only two cells in a reactive state. In contrast with previously reported studies our primary cultured microglia cultures did contain surveying or “resting” microglial cells. However, a possible mechanism for this diversity under control cells remains elusive. Since the same isolation and culture conditions were used, as reported by Boucsein *et al.* [19], we suggest that the induction of an equal amount of surveying and alerted control cells could be day-dependent, e.g. three days after plating, cells were brought back to the surveying state when no effective stimulus such as LPS was present. However, to confirm this, a cultivation study has to be performed. Additionally, we considered that the induction of a reactive phenotype was rather sporadic, since only 2 cells could be detected.

4.2 Minocycline-conditioning altered the I/V profile of primary cultured microglial cells

Further, in agreement with our hypothesis, we found that minocycline significantly reduced the K_{dr} current in LPS-activated cells. However, we also found that minocycline was able to significantly increase the K_{ir} current in LPS-activated and control cells which resulted in a “new” I/V profile. Since we accepted the presence of the K_{ir} current as a marker for microglial cells in an alerted state, we considered that this “new” minocycline-induced phenotype corresponded to that of microglia in an alerted state. Although the K_{ir} current in minocycline-conditioned LPS-activated cells was significantly higher than the alerted control cells, we considered this phenotype the same as alerted cells. In these cells, the K_{ir} current was already enlarged through the activation with LPS and seemed to be enforced via minocycline. Moreover, this new hypothesis was confirmed with the data that minocycline-conditioned cells tended to be in a depolarized state comparable to that of control alerted microglial cells. Since minocycline was able to induce this I/V profile and depolarized state both in control and

LPS-activated cells, the present study suggested that minocycline can bring microglial cells into an alerted state, independently of their activation history. However, a possible mechanism how minocycline induced this phenotype remains elusive. Since we considered the K_{ir} current to be a Kir2.1-like current and the K_{dr} current to be a Kv1.3 or Kv1.5-like current, we suggest that minocycline was able to exert its effects at the level of gene expression, by stimulating the functional expression of a Kir 2.1-like current and inhibiting the expression of the Kv1.3 and 1.5-like current. It has been described that minocycline has a suppressive effect on microglial transcription factors, such as mitogen-activated protein kinase (MAPK) and nuclear factor-kappaB (NF-KB), which are hallmarks of activated microglial cells and are critical for the expression of many inflammatory mediators, such as nitric oxide (NO), IL-6 and IL-1β [48, 49]. As reported by Nikodemova *et al.* [48], minocycline exerted its inhibitory effects on MAKP and the degradation of the inhibitory proteins of NF-KB in LPS-stimulated cells [48]. Also a study from Yang *et al.* [49] reported that minocycline was able to inhibit the LPS-mediated activation, whereby p38 MAPK was inhibited upon exposure to minocycline. Since we postulated the K_{dr} current to be a Kv1.3- and/or Kv1.5-like current, we hypothesized that the gene expression of Kv1.3 and/or Kv1.5 was also regulated by the p38 MAPK pathway and therefore got inhibited upon exposure to minocycline. Moreover, the Kir2.1-like current seemed to be upregulated upon exposure to minocycline, indicating that the gene expression of the Kir2.1 channel was not regulated via the p38-MAPK pathway, but instead was regulated via other transcription factors or pathways. One of those pathways could be the effect of minocycline on specific protein kinases or phosphatases. As reported by Hinard *et al.* [50], in human myoblast cells, the upregulation of the Kir2.1 channel activity was mediated through a dephosphorylation of the channel itself. Moreover, from a study of Zhu *et al.* [51], the activity of another inward rectifier channel (Kir2.3) seemed to be suppressed when protein kinase C was able to phosphorylate this channel. These facts indicated that minocycline could be able to inhibit specific kinases that keep the channel phosphorylated or activate phosphatases that can dephosphorylate the K_{ir} channel. In addition, further evidence that minocycline induced the K_{ir} current appears from a study in weaver mice, an animal model for Parkinson's disease. In this mice model, a mutation in the gene encoding the G-protein inwardly rectifying potassium channel Girk2 caused inflammation-mediated neurodegeneration. When minocycline was administrated, the neurodegeneration has been ameliorated [52]. These facts might indicate that the administration of minocycline was able to induce a K_{ir} current that replaced the absent K^+ current due to the Girk2-mutation and in that way counteracted the inflammation response. However, since minocycline was able to activate or to enforce the K_{ir} current, the exact function of this K_{ir} current in alerted and reactive cells still remains elusive and future experiments with specific blockers are needed to explore the functional roles of K_{ir} channels in microglial cells.

Furthermore, our results indicated that minocycline-conditioned microglial cells tended to be in a depolarized state and confirmed our hypothesis that the minocycline-induced phenotype was comparable to that of control alerted cells. Moreover, preliminary data have shown that minocycline itself was not responsible for this depolarizing effect, since the acute administration of minocycline did not induced an acute depolarization of the cell membrane of control microglial cells (data not shown). Therefore, we suggest that the depolarizing RMP in alerted control and minocycline-conditioned cells could also have its origin at the level of gene expression. Since the activation process in microglial cells is accompanied with an alteration in gene expression, alerted microglial cells express channels specific for their activation state. This hypothesis could be enforced with the data of the functional current-clamp experiments. As seen in figure 8 and 11, the current-clamp recordings of the alerted and minocycline-stimulated microglial cells showed unstable (fluctuating) current-clamp traces. This fluctuating profile might indicate that other channels, e.g. transient-receptor potential (TRP) channels, are activated in the alerted state that bring these cells to a depolarized state. Since it was reported that primary microglial cells can be activated by hypothermia and rewarming, we suggested the presence of temperature-sensitive TRP-channels on microglial cells. Moreover, a putative Ca^{2+}-increase due to subsequent ATP applications in BV-2 cells resulted in preliminary experiments with BV-2 cells in an increasing TRP-like current (data not shown). The cold-activation combined with the Ca^{2+}-sensitivity suggested the presence of the TRPA1 current in primary microglial cells. However, data have indicated that the TRPA1 channel was not present on the primary microglial cells (data not shown), but instead other TRP channels might be present. To investigate this further functional expression experiments have to be done.

Further, in contrast with our theory in figure 7, minocycline reduced the ATP-mediated membrane depolarization in the minocycline-conditioned cells. This small depolarization can be explained through the lower Ca^{2+} driving force in a depolarized state, indicating that less Ca^{2+} can flow into the cells when they were stimulated with ATP. Moreover, minocycline-conditioned cells also had a lower ATP-response, indicating that less Ca^{2+} flows into the cells when the ATP-mediated membrane depolarization was induced. This low ATP-response also might indicate that minocycline was able to inhibit the expression of the purinergic receptors. This was confirmed by Wixey *et al.*[53], since they had shown that minocycline was able to inhibit the expression of the P2X4 receptors.

In summary, these data indicated that minocycline was able to suppress the K_{dr} current in LPS-activated cells and to enforce the K_{ir} current in control and LPS-activated primary cultured microglial cells. Since we accepted the presence of this K_{ir} current for cells in an alerted state, accumulated with the high RMP in alerted and minocycline-conditioned cells, we suggested this “new” I/V profile to be

microglial cells in an alerted state. However, the exact mechanism how minocycline was responsible for these alterations still remains elusive and needs to be further investigated (Figure 17). Furthermore, our results indicated that minocycline-conditioned primary cultured microglial cells had a I/V profile comparable to that of the I/V profile of IL-4 stimulated BV-2 cells. This enabled us to extend our hypothesis, in which we claim that minocycline was able to bring microglial cells to an alerted activation state and changes the phenotype from a pro-inflammatory to an anti-inflammatory phenotype. Moreover, our results confirmed this hypothesis since minocycline-conditioned cells were able to suppress the production of pro-inflammatory cytokines, such as TNF-α and IL-6. Although our results indicated that minocycline was also able to suppress the secretion of the anti-inflammatory cytokine IL-10, we cannot state that our new hypothesis is not correct, since IL-10 was just one out of many anti-inflammatory cytokines (Figure 17).

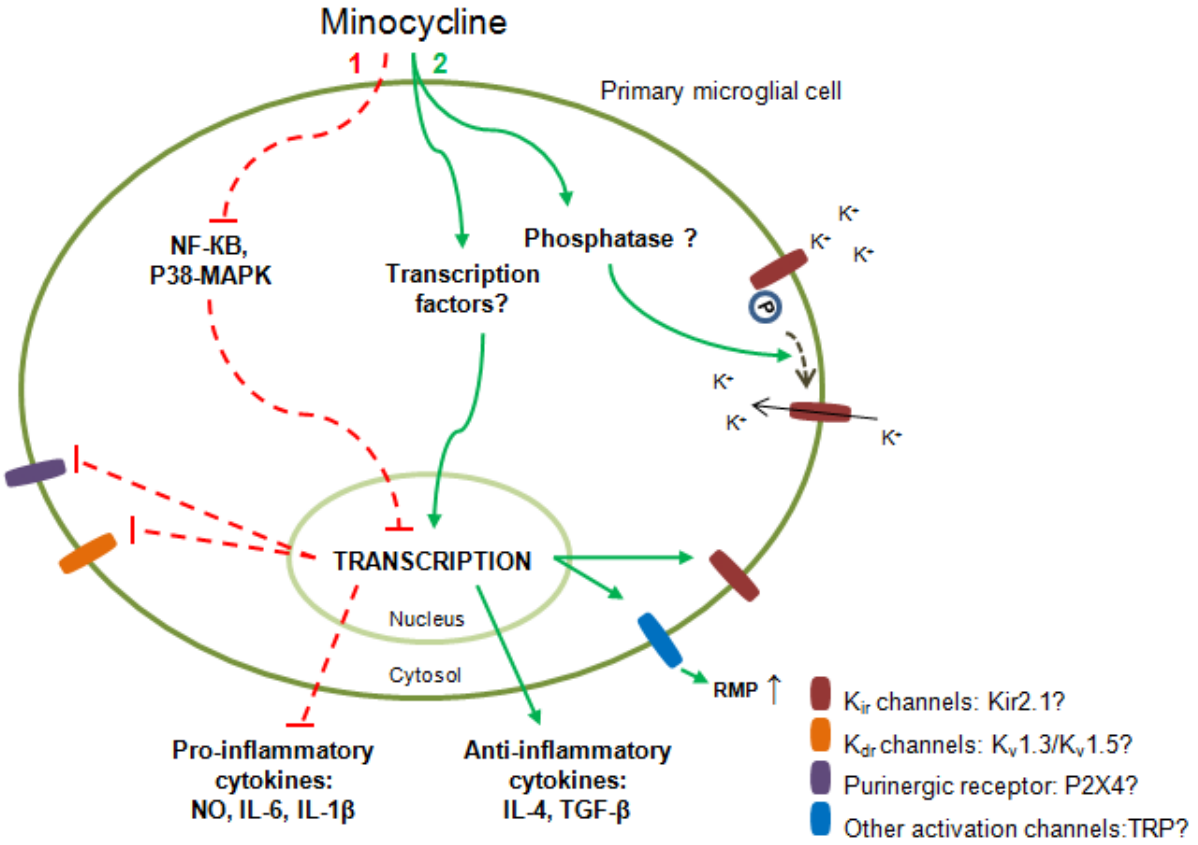

Figure 17. Overview of the possible working mechanism of minocycline on primary cultured rat microglial cells. The working mechanism of minocycline is likely to consist out of 2 complementary pathways. (1) Minocycline is likely to inhibit transcription factors (NF-KB and/or p38-MAPK) which eventually leads to the inhibition of transcription and functional expression of K_{dr} channels (Kv1.3 and/or Kv1.5), and purinergic receptors (P2X4). (2) Minocycline is likely to activate or to enforce the functional expression of K_{ir} channels and other channels linked to activation. The functional expression of K_{ir} channels can be regulated via the stimulation of phosphatases, which in turn dephosphorylate existing K_{ir} channels, or via transcription factors that induce the transcription of K_{ir} channels and/or other activation-linked channels, such as TRP channels, that lead to a depolarized RMP.

4.3 The electrophysiological profiling of microglial cells in situ

In a last part of the study, we performed a pilot study, where we studied the I/V relationship of microglial cells within brain slices to evaluate the working mechanism of minocycline in an animal model of MS. For this, we studied the I/V relationship of microglial cells in brain slices, within their natural micro-environment. We investigated the I/V relationships as indicated by Boucsein *et al.* [19] and in agreement with their results, we found that microglial cells in control animals showed a linear-like profile, indicating that they were in their surveying state. The microglial cells in the brain slices of EAE-induced animals, showed the profile of an alerted microglia (a K_{ir} current and a small K_{dr} current) and of a reactive microglia (a K_{ir} current and a prominent K_{dr} current). Outgoing from these results, reactive microglial cells are thus ideal targets to be inhibited through minocycline since they expressed the K_{dr} current in the mice induced with EAE. However, more experiments have to be performed to indicate whether this suppressive effect of minocycline on the K_{dr} current of primary cultured microglial cells (in vitro) is also represented on microglial cells in brain slices (in situ). Moreover, since we claimed that minocycline was able to bring control and LPS-activated microglial cells to an anti-inflammatory phenotype in vitro, this hypothesis also needs to be confirmed in vivo.

In summary, these data might indicate that the minocycline-induced reduction of the neuroinflammatory response in animal models of neurodegenerative diseases, such as MS and ALS, is likely to occur via the proposed mechanism of minocycline on the functional expression of potassium channels in microglial cells. However, to further explore the exact mechanism how minocycline exerts its effects on microglial cells, more experiments have to be done.

5. Conclusions and future perspectives

In this study, the results have indicated that in contrast with the literature, control cells can be classified into three groups, based on their I/V-profiles and current-clamp traces: surveying, alerted and reactive microglial cells. However, further cultivation studies have to be performed in order to elucidated the mechanism responsible for the induction of this diversity in control cells. Furthermore, our results also have indicated that minocycline was able to induce a **"new"** I/V profile, in which the K_{dr} current was suppressed in LPS-stimulated cells and the K_{ir} current was stimulated in control and LPS-stimulated cells. Since this "new" I/V profile and the depolarized RMP were comparable to that of alerted control cells, we suggested this "new" minocycline-induced phenotype to be microglial cells in an **alerted state**. Therefore, in contrast with our hypothesis, we suggested that minocycline was not able to fully inactivate reactive microglial cells, but instead brought surveying and reactive cells to an alerted state. Although minocycline-conditioned cells stimulated the K_{ir} current, the function of the K_{ir} current is not elucidated yet. This indicates that further experiments with specific blockers are needed to determine the function of these K_{ir} channels. Furthermore, since our results indicated that minocycline was able to induce a I/V-profile comparable to that of IL-4-conditioned BV-2 cells, together with the suppression of the production of pro-inflammatory cytokines (TNF-α and IL-6), we extended our hypothesis in which we claim that minocycline was able to bring microglial cells from a pro- to an **anti-inflammatory phenotype**. Although our results indicated that the production of IL-10 was reduced in minocycline-conditioned cells, further experiments, such as ELISA, PCR or immunohistochemical stainings are needed to confirm or reject this hypothesis. Finally, the data of our pilot study indicated that microglial cells in brain slices were ideal candidates to target them with minocycline. However, also further experiments are needed to reveal to working mechanism of minocycline as depicted in figure 17 and whether these results of minocycline-conditioning in vitro are also represented on minocycline-conditioned microglial cells in vivo.

This study has led to more insight into one of the major strategies in neurodegenerative diseases, namely the suppression of the microglia-mediated neuroinflammation. However, since this study only focused on microglial cells, the effect of minocycline on other immune cells, such as dendritic and T-cells, also has to be further explored. Eventually, further research in unraveling the working mechanism on microglial and other immune cells might lead to the development of more specific blockers that lead to future therapies in neuroinflammatory and neurodegenerative disease.

References

1. Allen, N.J. and B.A. Barres, *Neuroscience: Glia - more than just brain glue.* Nature, 2009. **457**(7230): p. 675-7.
2. Graeber, M.B. and W.J. Streit, *Microglia: biology and pathology.* Acta Neuropathol. **119**(1): p. 89-105.
3. Gonzalez-Scarano, F. and G. Baltuch, *Microglia as mediators of inflammatory and degenerative diseases.* Annu Rev Neurosci, 1999. **22**: p. 219-40.
4. Kreutzberg, G.W., *Microglia: a sensor for pathological events in the CNS.* Trends Neurosci, 1996. **19**(8): p. 312-8.
5. Frank-Cannon, T.C., et al., *Does neuroinflammation fan the flame in neurodegenerative diseases?* Mol Neurodegener, 2009. **4**: p. 47.
6. Streit, W.J., R.E. Mrak, and W.S. Griffin, *Microglia and neuroinflammation: a pathological perspective.* J Neuroinflammation, 2004. **1**(1): p. 14.
7. Schlachetzki, J.C. and M. Hull, *Microglial activation in Alzheimer's disease.* Curr Alzheimer Res, 2009. **6**(6): p. 554-63.
8. Yang, M.S., K.J. Min, and E. Joe, *Multiple mechanisms that prevent excessive brain inflammation.* J Neurosci Res, 2007. **85**(11): p. 2298-305.
9. Perry, V.H., C. Cunningham, and C. Holmes, *Systemic infections and inflammation affect chronic neurodegeneration.* Nat Rev Immunol, 2007. **7**(2): p. 161-7.
10. Napoli, I. and H. Neumann, *Protective effects of microglia in multiple sclerosis.* Exp Neurol, 2009.
11. Minghetti, L., *Role of inflammation in neurodegenerative diseases.* Curr Opin Neurol, 2005. **18**(3): p. 315-21.
12. Cuoghi, B. and L. Mola, *Macroglial cells of the teleost central nervous system: a survey of the main types.* Cell Tissue Res, 2009. **338**(3): p. 319-32.
13. Gee, J.R. and J.N. Keller, *Astrocytes: regulation of brain homeostasis via apolipoprotein E.* Int J Biochem Cell Biol, 2005. **37**(6): p. 1145-50.
14. Montgomery, D.L., *Astrocytes: form, functions, and roles in disease.* Vet Pathol, 1994. **31**(2): p. 145-67.
15. Saher, G. and M. Simons, *Cholesterol and myelin biogenesis.* Subcell Biochem. **51**: p. 489-508.
16. Kim, S.U. and J. de Vellis, *Microglia in health and disease.* J Neurosci Res, 2005. **81**(3): p. 302-13.
17. Pivneva, T.A., *Microglia in normal condition and pathology.* Fiziol Zh, 2008. **54**(5): p. 81-9.
18. Hanisch, U.K. and H. Kettenmann, *Microglia: active sensor and versatile effector cells in the normal and pathologic brain.* Nat Neurosci, 2007. **10**(11): p. 1387-94.
19. Boucsein, C., H. Kettenmann, and C. Nolte, *Electrophysiological properties of microglial cells in normal and pathologic rat brain slices.* Eur J Neurosci, 2000. **12**(6): p. 2049-58.
20. Pocock, J.M. and H. Kettenmann, *Neurotransmitter receptors on microglia.* Trends Neurosci, 2007. **30**(10): p. 527-35.
21. Pannasch, U., et al., *The potassium channels Kv1.5 and Kv1.3 modulate distinct functions of microglia.* Mol Cell Neurosci, 2006. **33**(4): p. 401-11.
22. Prinz, M., et al., *Microglial activation by components of gram-positive and -negative bacteria: distinct and common routes to the induction of ion channels and cytokines.* J Neuropathol Exp Neurol, 1999. **58**(10): p. 1078-89.
23. Hille, *Ion Channels of Excitable Membranes*. 3th ed. 2001: Sinauer Associates, Inc. 814.
24. Boron, B., ed. *Medical Physiology*. Updated-edition ed. 2005, Elsevier Saunders.
25. Eder, C., *Ion channels in microglia (brain macrophages).* Am J Physiol, 1998. **275**(2 Pt 1): p. C327-42.
26. Kettenmann, H., et al., *Cultured microglial cells have a distinct pattern of membrane channels different from peritoneal macrophages.* J Neurosci Res, 1990. **26**(3): p. 278-87.

27. Visentin, S., et al., *Ion channels in rat microglia and their different sensitivity to lipopolysaccharide and interferon-gamma.* J Neurosci Res, 1995. **42**(4): p. 439-51.
28. Draheim, H.J., et al., *Induction of potassium channels in mouse brain microglia: cells acquire responsiveness to pneumococcal cell wall components during late development.* Neuroscience, 1999. **89**(4): p. 1379-90.
29. Menteyne, A., et al., *Predominant functional expression of Kv1.3 by activated microglia of the hippocampus after Status epilepticus.* PLoS One, 2009. **4**(8): p. e6770.
30. Wickenden, A., *K(+) channels as therapeutic drug targets.* Pharmacol Ther, 2002. **94**(1-2): p. 157-82.
31. Ye, D., et al., *Current strategies for the discovery of K+ channel modulators.* Curr Top Med Chem, 2009. **9**(4): p. 348-61.
32. Uitdehaag, B.M., et al., *Effect of K+ channel blockers on the clinical course and histological features of experimental allergic encephalomyelitis.* Acta Neurol Scand, 1994. **90**(4): p. 299-301.
33. Smith, K.J., P.A. Felts, and G.R. John, *Effects of 4-aminopyridine on demyelinated axons, synapses and muscle tension.* Brain, 2000. **123 (Pt 1)**: p. 171-84.
34. Judge, S.I. and C.T. Bever, Jr., *Potassium channel blockers in multiple sclerosis: neuronal Kv channels and effects of symptomatic treatment.* Pharmacol Ther, 2006. **111**(1): p. 224-59.
35. Judge, S.I., et al., *Voltage-gated potassium channels in multiple sclerosis: Overview and new implications for treatment of central nervous system inflammation and degeneration.* J Rehabil Res Dev, 2006. **43**(1): p. 111-22.
36. Devasahayam, G., W.M. Scheld, and P.S. Hoffman, *Newer antibacterial drugs for a new century.* Expert Opin Investig Drugs. **19**(2): p. 215-34.
37. Yong, V.W., et al., *Experimental models of neuroprotection relevant to multiple sclerosis.* Neurology, 2007. **68**(22 Suppl 3): p. S32-7; discussion S43-54.
38. Zabad, R.K., et al., *The clinical response to minocycline in multiple sclerosis is accompanied by beneficial immune changes: a pilot study.* Mult Scler, 2007. **13**(4): p. 517-26.
39. Van Den Bosch, L., et al., *Minocycline delays disease onset and mortality in a transgenic model of ALS.* Neuroreport, 2002. **13**(8): p. 1067-70.
40. Kriz, J., M.D. Nguyen, and J.P. Julien, *Minocycline slows disease progression in a mouse model of amyotrophic lateral sclerosis.* Neurobiol Dis, 2002. **10**(3): p. 268-78.
41. Orsucci, D., et al., *Neuroprotective effects of tetracyclines: molecular targets, animal models and human disease.* CNS Neurol Disord Drug Targets, 2009. **8**(3): p. 222-31.
42. Henry, C.J., et al., *Minocycline attenuates lipopolysaccharide (LPS)-induced neuroinflammation, sickness behavior, and anhedonia.* J Neuroinflammation, 2008. **5**: p. 15.
43. Zhu, S., et al., *Minocycline inhibits cytochrome c release and delays progression of amyotrophic lateral sclerosis in mice.* Nature, 2002. **417**(6884): p. 74-8.
44. Maier, K., et al., *Multiple neuroprotective mechanisms of minocycline in autoimmune CNS inflammation.* Neurobiol Dis, 2007. **25**(3): p. 514-25.
45. Du, Y., et al., *Minocycline prevents nigrostriatal dopaminergic neurodegeneration in the MPTP model of Parkinson's disease.* Proc Natl Acad Sci U S A, 2001. **98**(25): p. 14669-74.
46. Stence, N., M. Waite, and M.E. Dailey, *Dynamics of microglial activation: a confocal time-lapse analysis in hippocampal slices.* Glia, 2001. **33**(3): p. 256-66.
47. Michelucci, A., et al., *Characterization of the microglial phenotype under specific pro-inflammatory and anti-inflammatory conditions: Effects of oligomeric and fibrillar amyloid-beta.* J Neuroimmunol, 2009. **210**(1-2): p. 3-12.
48. Nikodemova, M., I.D. Duncan, and J.J. Watters, *Minocycline exerts inhibitory effects on multiple mitogen-activated protein kinases and IkappaBalpha degradation in a stimulus-specific manner in microglia.* J Neurochem, 2006. **96**(2): p. 314-23.

49. Yang, L.P., X.A. Zhu, and M.O. Tso, *Minocycline and sulforaphane inhibited lipopolysaccharide-mediated retinal microglial activation.* Mol Vis, 2007. **13**: p. 1083-93.
50. Hinard, V., et al., *Initiation of human myoblast differentiation via dephosphorylation of Kir2.1 K+ channels at tyrosine 242.* Development, 2008. **135**(5): p. 859-67.
51. Zhu, G., et al., *Suppression of Kir2.3 activity by protein kinase C phosphorylation of the channel protein at threonine 53.* J Biol Chem, 1999. **274**(17): p. 11643-6.
52. Peng, J., et al., *Nigrostriatal dopaminergic neurodegeneration in the weaver mouse is mediated via neuroinflammation and alleviated by minocycline administration.* J Neurosci, 2006. **26**(45): p. 11644-51.
53. Wixey, J.A., et al., *Delayed P2X4R expression after hypoxia-ischemia is associated with microglia in the immature rat brain.* J Neuroimmunol, 2009. **212**(1-2): p. 35-43.

Auteursrechtelijke overeenkomst

Ik/wij verlenen het wereldwijde auteursrecht voor de ingediende eindverhandeling:
Minocycline-conditioning brings surveying and reactive microglial cells to an alerted state according to their potassium channel profile

Richting: **master in de biomedische wetenschappen-klinische moleculaire wetenschappen**
Jaar: **2010**

in alle mogelijke mediaformaten, - bestaande en in de toekomst te ontwikkelen - , aan de Universiteit Hasselt.

Niet tegenstaand deze toekenning van het auteursrecht aan de Universiteit Hasselt behoud ik als auteur het recht om de eindverhandeling, - in zijn geheel of gedeeltelijk -, vrij te reproduceren, (her)publiceren of distribueren zonder de toelating te moeten verkrijgen van de Universiteit Hasselt.

Ik bevestig dat de eindverhandeling mijn origineel werk is, en dat ik het recht heb om de rechten te verlenen die in deze overeenkomst worden beschreven. Ik verklaar tevens dat de eindverhandeling, naar mijn weten, het auteursrecht van anderen niet overtreedt.

Ik verklaar tevens dat ik voor het materiaal in de eindverhandeling dat beschermd wordt door het auteursrecht, de nodige toelatingen heb verkregen zodat ik deze ook aan de Universiteit Hasselt kan overdragen en dat dit duidelijk in de tekst en inhoud van de eindverhandeling werd genotificeerd.

Universiteit Hasselt zal mij als auteur(s) van de eindverhandeling identificeren en zal geen wijzigingen aanbrengen aan de eindverhandeling, uitgezonderd deze toegelaten door deze overeenkomst.

Voor akkoord,

Dries, Eef

Datum: **15/06/2010**